The Solvation of Acetonitrile

Jeffrey R. Reimers* and Lachlan E. Hall†

Contribution from the School of Chemistry, University of Sydney, NSW 2006, Australia

Received November 9, 1998. Revised Manuscript Received February 18, 1999

Abstract: Acetonitrile is an extremely important solvent and cosolvent. Despite this, we have no general picture of the nature of mixed liquids containing acetonitrile applicable across-solvent families. We consider the properties of acetonitrile dissolved in 33 solvents, focusing on interpretation of the environment-sensitive solvent shift, $\Delta\nu$, of its CN stretch frequency, ν_2. The two major models (dispersive and specific solvation) which have been proposed to interpret $\Delta\nu$ are based on diverse experiments with incompatible conclusions. We ascertain the robust features of these models and combine them into a new one in which solvent−solvent and solvent−solute forces compete to determine the structure of the solution and hence $\Delta\nu$. First, $\Delta\nu$ is analyzed in terms of solvent repulsive and dielectric effects combined with specific solvation effects. To interpret this specific solvation, 95 MP2 or B3LYP calculations are performed to evaluate structures and CN frequency shifts for CH_3CN complexed with one molecule of either water, methanol, ethanol, 2-propanol, *tert*-butyl alcohol, phenol, benzyl alcohol, acetic acid, trifluoroacetic acid, 2,2,2-trifluoroethanol, 1,1,1,3,3,3-hexafluoro-2-propanol, acetonitrile, chloroform, carbon tetrachloride, tetrahydrofuran, formamide, pyridine, or Cl^-, as well as 45 parallel calculations for the solvent monomers or dimers. The results are then convolved using known structural properties of the various solutions and/or related neat liquids, leading to an interpretation of the observed solvent shifts. Also, we measure $\Delta\nu$ for acetonitrile in aqueous solution using Fourier transform Raman spectroscopy and show that the results are consistent with, but require modification of, microheterogeneity theories for the structure of acetonitrile−water solutions. Although such theories are still in their infancy, we suggest that microheterogeneity could also account for most known properties of acetonitrile−alcohol solutions and, in fact, be a quite general phenomenon.

1. Introduction

Acetonitrile (ACN), both when neat and when mixed with, e.g., water (HOH), is a very commonly used solvent in which many hydrophobic and hydrophilic materials will dissolve. It is, however, becoming evident that the structural properties of liquids containing ACN are very complex.[1] Water−ACN mixtures exhibit anomalous thermodynamic properties, and this has led to the postulate of *microheterogeneity*,[2−4] in which the solution is thought to separate into regions of ACN and regions of water. Further, from the work of Eisenthal et al.,[5] ACN is known to form a thin layer at the liquid−air interface above aqueous solutions ordered akin to the surface of neat acetonitrile,[6] and here we present spectroscopic evidence for two types of ACN environments in aqueous solution. Mixtures of methanol (MeOH) and ACN also show similar effects,[7,8] with very dilute MeOH in ACN known to exist in tetramer or larger clusters, while very dilute ACN in MeOH is at least 20% uncomplexed by MeOH. Our analysis, presented herein, of spectroscopic data for dilute ACN in the notionally noncomplexing solvent chloroform ($CHCl_3$), as well as the strongly basic solvent pyridine (Py), suggests that subtle structural effects are also very important in these systems. In this paper, we develop the outline of a unified model which could quantitatively account for all of these observations, a physical picture for the solvation of acetonitrile.

Indeed, a vast amount of experimental data for ACN in solution is available. Here, we concentrate just on one very revealing data set, the change in frequency, $\Delta\nu$, of the CN stretch, ν_2, induced by solvation. Data are available for $\Delta\nu$ obtained in 33 solvents (including the neat liquid), and a large number of studies of this effect have been performed. Of these, the most thorough, recent, and/or relevant studies are those of Eaton, Pena-Nuñez, and Symons,[1] Ben-Amotz, Lee, Cho, and List,[9] and Fawcett, Liu, and Kessler.[10] Ben-Amotz et al.[9] consider $\Delta\nu$ in seven solvents as a function of concentration and pressure. Their results were interpreted in terms of a physically based model involving solvent "repulsive" and "attractive" interactions, and they concluded that no specific solvation effects are associated with hydrogen bonding. Fawcett et al.[10] consider $\Delta\nu$ for dilute ACN solutions in 26 solvents at atmospheric pressure. Contrary to the conclusions of Ben-Amotz et al., they concluded that $\Delta\nu$ is dominated by specific solvation effects, effects which correlate with Gutmann solvent donor

* To whom correspondence should be sent.

† Current address: Molecular Electronics Research, 393 Darling St., Balmain NSW 2041, Australia.

(1) Eaton, G.; Pena-Nuñez, A. S.; Symons, M. C. R. *J. Chem. Soc., Faraday Trans. 1* **1988**, *84*, 2181.

(2) Moreau, C.; Douhéret, G. *J. Chim. Phys.* **1974**, *71*, 1313.

(3) Kovacs, H.; Laaksonen, A. *J. Am. Chem. Soc.* **1991**, *113*, 5596.

(4) Marcus, Y.; Migron, Y. *J. Phys. Chem.* **1991**, *95*, 400.

(5) Zhang, D.; Gutow, J. H.; Eisenthal, K. B. *J. Chem. Phys.* **1993**, *98*, 5099.

(6) Case, B.; Hush, N. S.; Parsons, R.; Peover, M. E. *J. Electroanal. Chem.* **1965**, *10*, 360.

(7) Besnard, M.; Cabaço, M. I.; Strehle, F.; Yarwood, J. *Chem. Phys.* **1992**, *163*, 103.

(8) Farwaneh, S. S.; Yarwood, J.; Cabaço, I.; Besnard, M. *J. Mol. Liq.* **1993**, *56*, 317.

(9) Ben-Amotz, D.; Lee, M.-R.; Cho, S. Y.; List, D. J. *J. Chem. Phys.* **1992**, *96*, 8781.

(10) Fawcett, W. R.; Liu, G.; Kessler, T. E. *J. Phys. Chem.* **1993**, *97*, 9293.

(11) Gutmann, V. *Coord. Chem. Rev.* **1976**, *18*, 225.

10.1021/ja983878n CCC: $18.00
Published on Web 04/06/1999

Table 1. Properties of the Solvents Used

solvent	abbr	solvent property AN	DN	ϵ	n^2	μ_S	ρ_S	$\Delta\nu$ raw	corr
				Aprotic Solvents					
acetonitrile	ACN	18.9	14.1	37.5	1.7999	3.9	11.41	−13.0	−12.9
acetone	AC	12.5	17.0	20.7	1.8387	2.9	8.19	−13.5	−13.5
carbon tetrachloride	CCl_4	8.6	[0.0]	2.2	2.1319	0	6.23	−11.5	−11.2
methylene chloride	MeCl	20.4	[10]	9.1	2.0283	1.6	9.42	−12.0	−11.8
chloroform	$CHCl_3$	23.1	[10]	4.8	2.0906	1.0	7.45	−11.0	−10.7
toluene	MeBz	[10]	0.1	2.4	2.2383	0.4	5.63	−12.1	−11.9
nitromethane	NM	20.5	2.7	35.8	1.9033	3.5	11.22	−13.0	−12.9
formamide	F	39.8	24	111.0	2.0932	3.8	15.16	−12.5	−12.4
N-methylformamide	NMF	32.1	27	182.4	2.0449	3.8	10.31	−14.5	−14.6
propylene carbonate	PC	18.3	15.1	66.1	2.0190	5.0	7.01	−14.0	−14.0
dimethylformamide	DMF	16.0	26.6	36.7	2.0398	3.9	7.82	−15.5	−15.7
dimethylacetamide	DMA	13.6	27.8	37.8	2.0609	3.8	6.47	−16.5	−16.8
dimethyl sulfoxide	DMSO	19.3	29.8	46.7	2.1824	4.0	8.49	−17.5	−17.9
hexamethylphosphoramide	HMPA	10.6	38.8	30.0	2.1228	4.5	3.44	−18.5	−19.0
pyridine	Py	14.2	33.1	12.3	2.2786	2.2	7.48	−14.8	−14.9
tetrahydrofuran	THF	8.0	20.0	7.6	1.9740	1.6	7.44	−15.0	−15.2
benzene	Bz	8.2	[0.0]	2.3	2.2440	0	6.77	−13.0	−12.9
n-hexane	Hx	[0.0]	[0.0]	1.9	1.8820	0	4.62	−10.5	−10.1
cyclohexane	CHx	[0.0]	[0.0]	2.0	2.0352	0	5.57	−10.5	−10.1
nitrobenzene	NB	14.8	4.4	34.8	2.4060	4.3	5.89	−14.0	−14.0
diethyl ether	DEE	3.9	19.2	4.3	1.8295	1.1	5.80	−12.5	−12.4
benzonitrile	BN	15.5	11.9	25.2	2.3290	4.5	5.90	−14.0	−14.0
1,2-dichloroethane	DCE	16.7	0.0	10.4	2.0850	1.3	7.52	−13.0	−12.9
				Non-Fluorinated Alcohols and Water (ROH)					
water	HOH	54.8	18.0	78.3	1.7756	1.8	33.34	−6.7	−5.7
methanol	MeOH	41.3	19.0	32.7	1.7651	1.7	14.86	−7.5	−6.6
ethanol	EtOH	37.9	19.2	24.6	1.8480	1.7	10.32	−6.5	−5.5
2-propanol	PrOH	33.8	21.1	18.3	1.8910	1.7	7.87	−7.0	−6.0
tert-butyl alcohol	BuOH	27.1	21.9	10.8	1.9130	1.7	6.41	−7.0	−6.0
benzyl alcohol	BzOH	34.5	[20]	13.1	2.3704	1.7	5.80	−7.5	−6.6
				Poly-Fluorinated Alcohols					
2,2,2-trifluoroethanol	TFE	53.5	[10]	26.7[d]	1.6660[e]	2.0[g]	8.31	1.5	4.6
hexafluoro-2-propanol	HFIP	63.0	[10]	16.8[d]	1.6295[f]	2.0[g]	5.75[h]	9.5	17.4
				Acids					
acetic acid	AA	52.9	10	6.2	1.8813	1.7	10.52	−1.0	1.3
trifluoroacetic acid	TFAA	105.3	[10]	6.5	1.6460	2.3	8.10	12.5	19.4

[a−h] The ν_2 (CN stretch) solvent shift (in cm^{-1}) in raw form (*a* from ref 10, *b* from ref 9, *c* from ref 1, *d* this work) is the observed value less the gas-phase Q-branch value[14] of 2266.5 cm^{-1}; the corrected value is that as adjusted for Fermi resonance, see text. AN and DN are the solvent Gutmann acceptor and donor numbers, respectively; ϵ is the solvent dielectric constant; n is the solvent refractive index; μ_S is the solvent dipole moment, in D; and ρ_S is the solvent density, in nm^{-3}. Values for the solvent properties are taken from refs 10, 11, 22, 23, 86, and 87, except for *d*, ref 88, *e*, ref 89, *f*, ref 90, *g*, ref 91, and *h*, ref 92. Values enclosed in [] are estimates only; key results are insensitive to the values used.

numbers[11] and acceptor numbers.[12] Earlier, however, Eaton et al.[1] had performed a similar study using only nine solvents, but these solvents were more varied, and this group concluded, like Fawcett et al., that specific interactions are very important; however, they found the correlation with Gutmann descriptors to be actually quite poor. Further, they went on to interpret their results in terms of postulated complex solvent structure, and it is their line of thinking which is developed in this work. The genesis of these ideas can also be found in the 1978 review of Michel and Lippert.[13]

First, in section 2, we review the available experimental data. Next, we investigate, in detail, the analyses of Ben-Amotz et al.[9] (section 3) and Fawcett et al.[10] (section 4). These models have implications beyond their application to acetonitrile, and we demonstrate that, based on the individual experimental results analyzed within each paper, some of the conclusions drawn are not valid. Further, we isolate those of the conclusions which are robust and hence what features must be retained in an all-encompassing theory, and one such theory is shaped in section 5. This involves the separation of the observed solvent shift into contributions arising from continuum effects such as dispersion and solvent compression, with the remainder identified as specific solvation effects. Ab initio and density functional calculations are then performed in order to determine specific solvation effects in various acetonitrile complexes with 19 different sample solvent molecules. Last, in section 6, the observed and dimer-specific solvation effects are rationalized in terms of known structural properties of acetonitrile solutions and/or pure solvents.

2. Review of the Observed Solvent Shift Data

For ACN, ν_2 has been measured in (at least) 33 solvents at atmospheric pressure, and the observed solvent shifts (relative to the gas-phase ACN Q-branch absorption maximum[14,15] at 2266.5 cm^{-1}) are listed in Table 1, along with abbreviated names and key physical properties of each of the solvents used. Most

(12) Mayer, U.; Gutmann, V.; Gerger, W. *Monatsh. Chem.* **1975**, *106*, 1235.

(13) Michel, H.; Lippert, E. In *Organic liquids: structure, dynamics, and chemical properties*; Buckingham, A. D., Lippert, E., Bratos, S., Eds.; Wiley: New York, NY, 1978; p 293.

(14) Duncan, J. L.; McKean, D. C.; Tullini, F.; Nivellini, G. D.; Perez Peña, J. *J. Mol. Spectrosc.* **1978**, *69*, 123.

(15) Nishio, M.; Paillous, P.; Khlifi, M.; Bruston, P.; Raulin, F. *Spectrochim. Acta* **1995**, *51A*, 167.

Table 2. Variation in the Observed Raw Frequency Shift $\Delta\nu$ for ν_2 of ACN in Solution, in cm^{-1}

	ref[a]				
solvent	1986	1988	1990	1992	1993
ACN[b]	−14.0			−13.3	−13.0
AC			−13.8	−13.2	−13.5
CCl_4	−11.0	−10.6	−12.2	−11.2	−11.5
MeCl	−13.0		−12.5	−11.1	−12.0
$CHCl_3$	−12.0	−10.2	−11.5	−9.5	−11.0
DMSO	−17.5	−17.3			−17.5
HMPA	−16.5				−18.5
Py	−14.5	−14.8			
Bz	−14.0	−12.9	−14.0		−13.0
MeOH			−9.1	−9.2	−7.5

[a] 1986: Bertran and Serna[17] FTIR on samples of 1% ACN mole fraction. 1888: McKean and Machray[18] FTIR on samples of 5% ACN mole fraction. 1990: Nyquist[16] FTIR on samples of 1% ACN mole fraction. 1992: Ben-Amotz at al.[9] Raman, extrapolated from samples of 5−100% ACN mole fraction. 1993: Fawcett et al.[10] FTIR on samples of 8.7% ACN mole fraction. [b] This work, −13.3 cm^{-1} from FT-Raman.

of these frequency shifts are taken from Fawcett et al.,[10] this being the most extensive collection of data obtained under the same conditions. Others are taken from either the works of Ben-Amotz et al.,[9] Eaton et al.,[1] or this work, as described later. Table 2 indicates the variability in the observed frequencies obtained using different methods: the largest variation is 2.0 cm^{-1} for HMPA, while the next largest is 1.7 cm^{-1} for MeOH. For MeOH, the source of the variation is easily identified: the spectra of Nyquist[16] and Ben-Amotz et al.[9] do not resolve ν_2 into its two components (such splitting occurs when ACN is dissolved in hydroxylic solvents[10]). Nevertheless, for the molecules shown in Table 2, the average root-mean-square (RMS) deviation is found to be 1 cm^{-1}, a value which can be regarded as the uncertainty in the experimental data.

Interpretation of the observed solvent shifts is also hampered by the effects of a *Fermi resonance* between ν_2 and the close-lying overtone $\nu_3 + \nu_4$. This arises as the frequency of ν_2 ($\sim$2170 cm^{-1}) is very similar to the sum of the frequencies[14] for the CCH bend, $\nu_3 = 1390$ cm^{-1}, and the CC stretch, $\nu_4 = 920$ cm^{-1}. Hence, these vibrational motions interfere (called "Fermi resonance"), with the consequence that ν_2 is pushed to lower frequency while the usually forbidden overtone band $\nu_3 + \nu_4 \sim 2300$ cm^{-1} becomes significantly intensified. Quantitatively, in the gas phase, the interaction strength is usually[14] taken as $W = 12$ cm^{-1}, and the observed bands at 2266.5 and 2305.4 cm^{-1} are interpreted as arising from unperturbed bands at 2270.6 (ν_2) and 2301.3 cm^{-1} ($\nu_3 + \nu_4$), respectively.

Solvation affects ν_2 more than $\nu_3 + \nu_4$ and hence modulates the Fermi resonance; its effects thus must be removed from the observed data in order to obtain the part of the frequency shift which is due to solvation alone. This has been done accurately for eight solvents (see Table 2) by Bertran and La Serna[17] and by McKean and Machray.[18] Unfortunately, insufficient data are available to extend these analyses to all of the molecules considered herein, and so we use a simpler, more general approach. It appears[18] that, in nonacidic solvents at least, the resonance interaction W is not modified by solvation (less accurate estimates place this interaction between[16,17] 16 and 18 cm^{-1}). To estimate Fermi resonance corrections to the observed solvent shift for all solvents, we assume that the unperturbed value of $\nu_3 + \nu_4$ in all solvents is 2288 cm^{-1} and that $W = 12$ cm^{-1}. This allows the conversion of the observed perturbed ν_2 to its unperturbed value and predicts also the observed value of $\nu_3 + \nu_4$ and its relative intensity. We find that the error in the actual $\nu_3 + \nu_4$ observed frequency (in eight solvents) obtained using this approach is 2 cm^{-1}, implying an uncertainty of 0.2 cm^{-1} in the unperturbed value of ν_2. From published spectra[10] for AA and TFAA, it is possible to crudely estimate W and the unperturbed frequencies. The results obtained for AA agree with those obtained from the above simple model, while those for TFAA do not. For TFAA, this crude analysis gives $W = 14$ cm^{-1} and unperturbed frequencies of 2290 and 2295 cm^{-1}; the near resonance in this case has a profound effect on the perceived solvent shift.

3. Physically Based Solvent Effect Model of Ben-Amotz et al.

Ben-Amotz et al.[9] have modeled the effects of seven solvents (see Table 2) on the (Fermi resonance uncorrected) frequency of the ν_1 (CH stretch), ν_2, and ν_4 (CC stretch) modes of ACN. They obtained and modeled detailed data for these solutions as a function of pressure and concentration. All of the parameters in their model involve consideration of the mean solvent−solute forces and include short-range repulsive ($\Delta\nu_R$) forces, long-range attractive ($\Delta\nu_A$) forces, and centrifugal distortion effects ($\Delta\nu_C$). They express the total solvent shift $\Delta\nu$ as

$$\Delta\nu = \Delta\nu_A + \Delta\nu_R + \Delta\nu_C \qquad (1)$$

The centrifugal term arises as, in the gas phase, ACN rotates, and thus there occurs a centrifugal distortion of the molecule which shifts the gas-phase vibration frequency. Ben-Amotz et al.[9] conclude that the inhibition of free rotation in solution results in a red shift of ν_2 by 0.5 cm^{-1}.

Short-range repulsive forces arise from collisions between the solvent and solute molecules; they are treated by Ben-Amotz et al.[9] using a hard-sphere model for the fluid and, at atmospheric pressure, are calculated to provide a uniform blue shift of ν_2 of 4.2 ± 0.5 cm^{-1}. This term dominates the solvent shift at high density and, based on Ben-Amotz et al.'s observed pressure dependence of $\Delta\nu$, appears well represented. Another study which measures the solvent shift under high pressure is that of Akimoto and Kajimoto[19] in supercritical Ar, CO_2, CF_3-Cl, and CF_3H.

For the long-range attractive interactions, Ben-Amotz et al.[9] consider the electrostatic interactions between the solute dipole μ_0 and the solvent dipole μ_S as well as the dispersive interaction between the solute polarizability α_0 and the solvent polarizability α_S. In absolute terms, the range of the electrostatic interactions is quite large, extending over 10 Å in length, while the dispersion terms decay much faster and span only the first and possibly second coordination spheres; both are much "longer range" than the "short-range" interactions, however, which decrease exponentially over sub-angstrom distances. The "long-range" term is thus expressed as

$$\Delta\nu_A = A_\mu \rho_S {\mu_S}^2 + A_\alpha \rho_S \alpha_S \qquad (2)$$

where ρ_S is the solvent density. By plotting $\Delta\nu_A/\rho_S$ as a function of ${\mu_S}^2$, Ben-Amotz et al.[9] deduced values of the coefficients of $A_\mu = -0.033 \pm 0.01$ cm^{-1} nm^3 D^{-2} and $A_\alpha = -226 \pm 15$

(16) Nyquist, R. A. *Appl. Spectrosc.* **1990**, *44*, 1405.
(17) Bertran, J. F.; La Serna, B. *Spectrochim. Acta* **1986**, *42A*, 955.
(18) McKean, D. C.; Machray, S. *Spectrochim. Acta* **1988**, *44A*, 533.
(19) Akimoto, S.; Kajimoto, O. *Chem. Phys. Lett.* **1993**, *209*, 263.
(20) Reimers, J. R.; Zeng, J.; Hush, N. S. *J. Phys. Chem.* **1996**, *100*, 1498.
(21) Stratt, R. M.; Adams, J. E. *J. Chem. Phys.* **1993**, *99*, 775.
(22) Fawcett, W. R. In *Quantitative treatment of solule/solvent interactions*; Politzer, P., Murray, J. S., Eds.; Elsevier: New York, NY, 1994; p 183.

cm^{-1}. By directly fitting these coefficients to minimize the RMS error, we obtain results of $A_\mu = -0.040$ cm^{-1} nm^3 D^{-2} and $A_\alpha = -220$ cm^{-1}, within their stated error range. The RMS error thus minimized is 1.2 cm^{-1}; however, this is very large when compared to the range of solvent shifts found in their seven solvents, just 4.1 cm^{-1}, and the maximum error in the fit is 2.1 cm^{-1}, or ca. 50%. Their model is thus not able to describe the attractive interactions as adequately as it does the repulsive ones.

Ben-Amotz et al.[9] interpret the solute properties A_μ and A_α using

$$A_\mu = \frac{16}{9k_\beta T}\mu_0\Delta\mu \qquad \text{and} \qquad A_\alpha = \frac{2\pi I_a}{\sigma_a^{\,3}}\Delta\alpha \tag{3}$$

where $\Delta\mu$ and $\Delta\alpha$ are the change in the solute dipole moment and polarizability accompanying the $0 \rightarrow 1$ vibrational transition in the CN stretch, k_β is Boltzman's constant, T is the temperature, I_a is the reduced ionization energy (set to 46 000 $\pm$ 3000 cm^{-1}), and σ_a is the average distance between a solvent and solute molecule (set to 4.5 $\pm$ 0.3 Å). To evaluate these expressions, Ben-Amotz et al.[9] introduce the linear approximations

$$\Delta\mu = m_1\Delta r \qquad \text{and} \qquad \Delta\alpha = \alpha_1\Delta r \tag{4}$$

to $\Delta\mu$ and $\Delta\alpha$, where Δr is the change in the expectation value of the CN bond length on excitation, and m_1 and α_1 are the dipole and polarizability derivatives in the direction of bond extension. These expressions evaluate to give[9] $A_\mu = -0.14$ cm^{-1} nm^3 D^{-2} and $A_\alpha = -96$ cm^{-1}, values which differ from the best-fit ones by factors of ca. 4 and 0.4, respectively. Further, direct use of eqs 1−4 to predict the absolute frequency shifts on the basis of the known microscopic physical properties results in a maximum error of 12.3 cm^{-1} and a RMS error of 6.8 cm^{-1}, both much larger that the observed range in the experimental data.

We considered means by which both the interpretation of the coefficients (eqs 3 and 4) and the general description of the attractive contribution (eq 2) could be improved. First, the linear expansion of the parameters in eq 4 is known[20] to be inadequate for CN stretch vibrations: for $\Delta\mu$, the linear and quadratic terms are of equal magnitude and opposite sign, making the a priori evaluation of this quantity rather difficult. Instead, we employed a second-order expansion,[20] but the quality of the results did not improve. Similarly, we investigated extension of eq 2 by addition of solvent and solute polarization terms to the electrostatic interaction and higher order dispersion terms, thus introducing cross-terms between the μ_S and α_S dependencies. However, this required the evaluation of many more parameters, and it was considered that these could not be reliably extracted from the data set available for credible results to be produced.

More fundamentally, the approach of Ben-Amotz et al.[9] to modeling the long-range attractive contributions has two serious shortcomings: first, it does not allow for the possibility of specific solvent−solute interactions, and second, it does not allow for solvent−solvent interactions.

Specific solvent−solute interactions, such as hydrogen bonding, can induce relatively large vibrational frequency changes. From their results, Ben-Amotz et al.[9] found no evidence to suggest that such effects were operative. This conclusion is incorrect, as a more thorough analysis of the experimental data shows.[1,10] Also, their experimental results for MeOH were not sufficiently accurate for the gross specific solvation effects seen by other workers (see, e.g., refs 1 and 10) to be immediately obvious.

Solvent−solvent interactions can also be very important, especially if the solvent is polar. In their derivation of eqs 2 and 3, Ben-Amotz et al.[9] start with the interaction of a solute molecule with one solvent molecule and integrate over all possible locations of the solvent molecule, ignoring the contribution of solvent−solvent interactions to the liquid structure. For the closely related problem of the contribution of dispersive interactions to the shift of electronic spectral lines for molecules in rare gas matrixes, this approximation is known to be inadequate.[21] It ignores solvent−solvent interactions and the entropy of the system.

4. Solvent Descriptor Model of Fawcett et al.

Fawcett et al.[10] have considered the solvent shift of ν_2 in 26 solvents at atmospheric pressure. They conclude that the major contribution to the variation observed for ν_2 between different solvents arises from specific solvent−solute interactions. In its most general form,[22] their approach involves the fitting of the observed solvent shifts $\Delta\nu_2(S)$ for solvent S to a function containing four adjustable parameters:

$$\Delta\nu_2(S) = \Delta\nu_2(ACN) + [AN(S) - AN(ACN)]A_A + [DN(S) - DN(ACN)]A_D + [D(S) - D(ACN)]A_\epsilon + [P(S) - P(ACN)]A_\alpha \tag{5}$$

where AN is the Gutmann solvent *acceptor number*,[12] DN is the solvent Gutmann *donor number*,[11] D is indicative of the solvent dielectric strength,

$$D = \frac{\epsilon - 1}{\epsilon + 2} \tag{6}$$

where ϵ is the solvent dielectric constant, P is indicative of the solvent polarizability,

$$P = \rho_S\alpha_S = \frac{3}{4\pi}\frac{n^2 - 1}{n^2 + 1} \tag{7}$$

where n is the solvent's refractive index (this expression for the solvent polarizability is also used by Ben-Amotz et al.), and the fitted coefficients A_A, A_D, A_ϵ, and A_α reflect solute properties. Note that it is necessary to reference this fitting to the results for ACN as values for the empirical solvent descriptors AN and DN are not available for the gas phase.

The approach of Ben-Amotz et al. to interpreting solvent shifts in terms of solvent descriptors, is, of course, not unique, and investigation of alternate approaches (see, e.g., ref 22) may be worthwhile. Here, we concentrate specifically on Fawcett et al.'s approach as it has been applied to acetonitrile.[10,22] We use their terminology throughout, a terminology which is standard chemical practice.[11,22,23] Before examining quantitative performance, we first note some pedagogical issues. First, the DN are determined not from the properties of the molecular solvents but rather from the properties of the solvent molecules *as solutes*, suggesting that they would not be optimal solvent descriptors. Also, we note that, in the derivation by Fawcett et al., the AN are NMR shifts, in ppm, while the DN are heats of formation, in kcal mol^{-1}, not dimensionless numbers as usually[10,11,22,23] (and here) they are taken to be.

Our 33-molecule data set is partitioned into four subsets comprising the aprotic solvents, water and the non-fluorinated alcohols (ROH), the poly-fluorinated alcohols, and the carboxy-

(23) Gutmann, V.; Resch, G.; Linert, W. *Coord. Chem. Rev.* **1982**, *43*, 133.

Table 3. The Error in the Fit for Each Included Molecule, as Well as the Root Mean Square (RMS) Error and the Optimized Parameters for Fits A−C Obtained Using Eq 5, in cm^{-1} (See Text)

	fit				fit		
	A	B	C		A	B	C
ACN	[0]	[0]	0.5	NB	−2.4	−0.9	−3.4
AC	−1.2	−0.4	1.1	DEE	−1.2	−0.9	2.3
CCl_4	1.4	0.4	0.0	BN	−2.0	−1.1	−2.7
MeCl	0.6	−0.5	−1.4	DCE	0.5	0.8	−1.0
$CHCl_3$	1.9	−0.7	−2.0	HOH	3.4		
MeBz	1.7	0.7	−0.3	MeOH	0.7		
NM	0.6	0.9	−0.4	EtOH	−1.7		
F	3.3	−0.7	−3.0	PrOH	−2.3		
NMF	3.1	0.5	−0.4	BuOH	−3.6		
PC	−0.6	−0.2	−0.6	BzOH	−3.1		
DMF	0.0	0.0	1.1	AA	−0.6		
DMA	0.1	0.6	2.0	TFAA	−1.3		
DMSO	2.2	1.6	2.0				
HMPA	0.7	1.1	3.8	RMS	1.8	0.9	1.8
Py	−1.3	−1.9	−0.7	A_A	0.3099	0.1197	[0]
THF	0.3	0.8	2.7	A_D	−0.0556	−0.1049	[0]
Bz	2.4	1.6	0.8	A_ϵ	−11.30	−5.30	−6.62
Hx	−0.5	−0.3	1.5	A_α	−26.46	−23.37	−47.32
CHx	−1.6	−1.1	0.0				

lic acids, as detailed in Table 1. Three different fits, labeled A, B, and C, of the coefficients A_A, A_D, A_ϵ, and A_α have been performed, and the results are shown in Table 3 and Figure 1. Table 3 contains, for each molecule included in the fitting, the final error between the observed and fitted solvent shift, the values of the four deduced parameters, and the RMS error, while the figure shows the calculated shift from eq 5 as a function of the observed shift for all 33 molecules.

In fit A, all four parameters are adjusted to reproduce the Fermi resonance-corrected solvent shifts for the aprotic, ROH, and acidic solvents only. This data set forms just a minor extension of that used by Fawcett et al.[10,22] and contains no molecules with qualitatively different properties. The results appear quite impressive, with a standard deviation in the fit being just 1.9 cm^{-1}, or 5% of the observed range of $\Delta\nu$. This error is only slightly larger than the variability of the raw observed data, as detailed in Table 2, and a similar error is also appropriate for the Fermi resonance correction term. From the plot of observed versus fitted solvent shift shown in Figure 1, we see that the aprotic, hydroxylic, and acidic solvents behave quite differently from each other. Analysis of the relative contributions in eq 5 leads to the conclusion drawn by Fawcett et al.[10] that the solvent shift is controlled primarily by the solvent acceptor number, the property which most clearly distinguishes between the aprotic, hydroxylic, and acidic solvents.

However, also shown in Figure 1 are the predicted values for the two poly-fluorinated alcohols 2,2,2-trifluoroethanol (FTE) and 1,1,1,3,3,3-hexafluoro-2-propanol (HFIP) obtained by applying eq 5 using the coefficients from fit A. Very poor correlation is seen, and the results are not significantly improved by the inclusion of these molecules in the data set and reoptimizing the coefficients. Fawcett et al.[10] did not consider these solvents; several years earlier, Eaton et al.[1] had considered them and concluded, contrary to the conclusions of Fawcett et al., that the observed solvent shift correlated only poorly with solvent donor and acceptor numbers. Interestingly, solvent shifts for the CN stretch of CN^- do correlate well with the solvent acceptor number,[24] a result attributable to the much simpler nature of this ion.

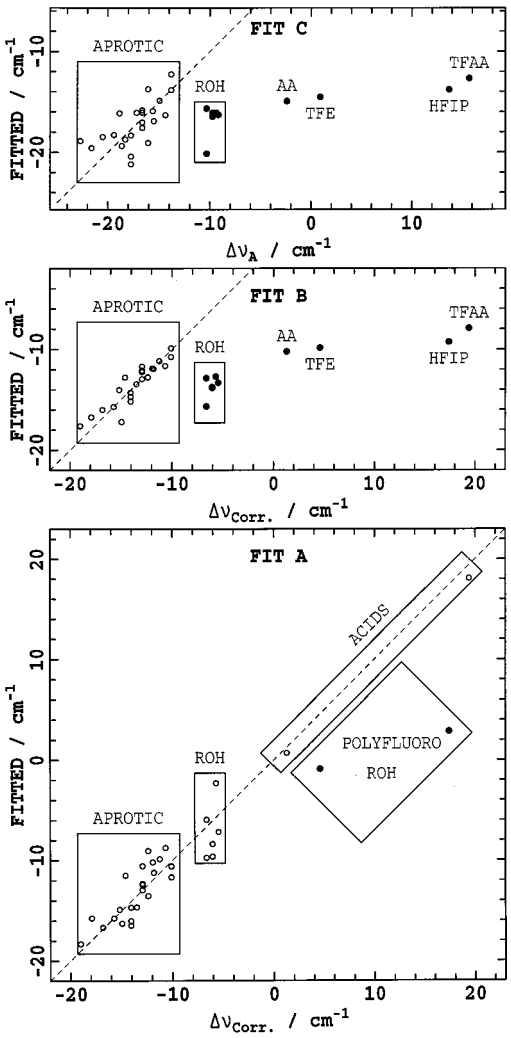

Figure 1. Plots of the fitted versus observed solvent shifts for the CN stretch of acetonitrile. $\Delta\nu_{Corr.}$ is the Fermi resonance-corrected gas-phase solvent shift from Table 1, while $\Delta\nu_A$ (eq 1, Table 4) is that corrected by -3.7 cm^{-1} to account for repulsive ($+4.2$ cm^{-1}) and centrifugal (-0.5 cm^{-1}) contributions to isolate the attractive and specific interaction contributions to the solvent shift. ○, used in the fitting; ●, not used in the fitting.

Further, it is possible to demonstrate, using only the data set employed in fit A, that quantitative analysis is not possible in terms of solvent donor and acceptor numbers. Fit B is constructed analogously to fit A except that only data for the 23 aprotic solvents are used in constructing the fit. Again, a very good fit to the data is produced (see Table 3), with a standard deviation of just 0.9 cm^{-1}, but the resulting coefficients change considerably from those obtained in fit A ($A_A \times 0.38$, $A_D \times 1.9$, $A_\epsilon \times 0.47$, and $A_\alpha \times 0.88$). Only the dispersive contribution appears robust, and, while donor and acceptor numbers are capable of qualitatively discriminating *between* the aprotic, hydroxylic, and acidic subsets, they clearly cannot quantitatively discriminate *within* the subsets. Figure 1, in which the ROH solvents are found to have approximately the same solvent shift independent of their donor numbers, indicates this also, as does a close scrutiny of Figure 5 from ref 10. Most importantly though, as shown in Figure 1, the parameters from fit B are completely inadequate for the prediction of the solvent shift of the hydroxylic and acidic solvents.

(24) Eaton, G.; Pena-Nuñez, A. S.; Symons, M. C. R.; Ferrario, M.; McDonald, I. R. *J. Chem. Soc., Faraday Discuss.* **1988**, *85*, 237.

(25) Reimers, J. R.; Watts, R. O. *Chem. Phys.* **1984**, *91*, 201.

Table 4. The Attractive Solvent Shift $\Delta\nu_A$ (Obtained as the Fermi Resonance-Corrected Solvent Shift from the Gas Phase with, for All Solvents, $\Delta\nu_R = +4.2$ cm^{-1} Repulsive and $\Delta\nu_C = -0.5$ cm^{-1} Centrifugal Correction) Partitioned into Electrostatic ($D(S)A_\epsilon$), Dispersive ($P(S)A_\alpha$), and Specific Solvation Contributions (See Eqs 5−7)

solvent	$\Delta\nu_A$	$D(S)A_\epsilon$	$P(S)A_\alpha$	specific	solvent	$\Delta\nu_A$	$D(S)A_\epsilon$	$P(S)A_\alpha$	specific	solvent	$\Delta\nu_A$	$D(S)A_\epsilon$	$P(S)A_\alpha$	specific
ACN	−16.6	−6.1	−10.0	−0.5	DMA	−20.5	−6.1	−12.4	−2.0	DCE	−16.6	−5.0	−12.6	1.0
AC	−17.2	−5.7	−10.3	−1.1	DMSO	−21.6	−6.2	−13.4	−2.0	HOH	−9.4	−6.4	−9.7	6.7
CCl_4	−14.9	−1.9	−13.0	0.0	HMPA	−22.7	−6.0	−12.9	−3.8	MeOH	−10.3	−6.0	−9.6	5.3
MeCl	−15.5	−4.8	−12.1	1.4	Py	−18.6	−5.2	−14.1	0.7	EtOH	−9.2	−5.9	−10.4	7.1
$CHCl_3$	−14.4	−3.7	−12.6	2.0	THF	−18.9	−4.6	−11.6	−2.7	PrOH	−9.7	−5.6	−10.8	6.7
MeBz	−15.6	−2.1	−13.8	0.3	Bz	−16.6	−2.0	−13.9	−0.8	BuOH	−9.7	−5.1	−11.0	6.4
NM	−16.6	−6.1	−11.0	0.4	Hx	−13.8	−1.5	−10.8	−1.5	BzOH	−10.3	−5.3	−14.8	9.8
F	−16.1	−6.4	−12.6	3.0	CHx	−13.8	−1.7	−12.1	0.0	TFE	0.9	−5.9	−8.6	15.4
NMF	−18.3	−6.5	−12.2	0.4	NB	−17.7	−6.1	−15.1	3.4	HFIP	13.7	−5.6	−8.2	27.5
PC	−17.7	−6.3	−12.0	0.6	DEE	−16.1	−3.5	−10.3	−2.3	AA	−2.4	−4.2	−10.7	12.5
DMF	−19.4	−6.1	−12.2	−1.1	BN	−17.7	−5.9	−14.5	2.7	TFAA	15.7	−4.3	−8.4	28.4

5. Shaping a Quantitative Theory

Our view is that, at the current time, it is not feasible to implement a quantitative computational scheme to model the solvent shift of ν_2 of acetonitrile in 33 solvents (possibly also as a function of concentration and temperature). However, we detail here the key physical features that are required in such a theory. The analysis of Ben-Amotz et al.[9] shows the importance of the dispersion and electrostatic interactions and the need to adequately model the repulsive contributions in order to understand the pressure dependence of the solvent shift. Clearly, these features must be included. Also, Fawcett et al.[10] have demonstrated the importance of specific solvent−solute interactions, and these must also be included. The key to their evaluation, however, is in the application of principles postulated by Michel and Lippert[13] and also by Eaton et al.:[1] it is the structure of the solvent molecules adjacent to the chromophore which, when combined with the intermolecular interactions, determines the extent of the specific solvation effect. We proceed in this section first by extracting an estimate of the magnitude of the specific solvation effects from the observed data, and then by considering ab initio the solvent shift arising from the intermolecular interactions between acetonitrile and single solvent molecules. The results are combined in the next section with existing knowledge concerning solution structures, resulting in a semiquantitative description of the observed solvent shifts.

Our approach is designed to minimize empiricism in the analysis of the experimental solvent shifts. Indeed, all of the empirical elements are contained in section 5a, where nonspecific contributions to the observed solvent shift are isolated and removed. These nonspecific effects would be all that is required if the solvent had no structure, and our method for extracting them essentially averages the specific (solvent structure-dependent) interactions over all solvents used in the data set. Removing the nonspecific contributions then gives the specific contribution, that which is taken to arises because the solvent is structured around the solute. Generally, we assume that this correlation extends only to two-body terms, i.e., can be interpreted in terms of prevalent complexes between the solute and just one solvent molecule. The ab initio calculations then consider a set of structures, at least one of which is likely to be resemble the prevalent liquid structure. We determine, from energetic or independent experimental evidence, which of these structures is the most likely and correlate the "observed" specific solvation effect with the solvent shift calculated for that cluster. This approach is immediately applicable if the vibrational transition is *inhomogeneously* broadened, a likely result for hydrogen-bonded systems, with, e.g., the OH vibrational spectrum of liquid water being *quantitatively* predictable[25] at this level. Other systems, however, could be *homogeneously* broadened with the liquid structure changing on the time scale of the frequency measurement. In this case, the observed vibration frequency would be intermediate between the frequencies calculated for the limiting structures, and our calculations should again lead to a qualitative interpretation of the observed solvent shift.

A point to note is that the calculated cluster frequency shifts contain contributions from (especially) dispersion which, in principle, is also included in the nonspecific interaction term. Hence, a small amount of double counting occurs, with this amount being related to the volume of the solvent molecule. In water, for which the nearest-neighbor coordination is 19,[26] this double counting is very small, but it could become more significant for larger solvent molecules. The possibility that more than one molecule is simultaneously involved in specific interactions with the solute is real; we discuss such possibilities, when appropriate, assuming that they are additive. Double counting is a more significant issue in those cases.

a. "Observed" Specific Solvation Magnitudes. The identified nonspecific interaction terms are the centrifugal shift $\Delta\nu_C$, the repulsive shift $\Delta\nu_R$, the dispersive contribution (through A_α), and an electrostatic contribution, representable in slightly different ways through either A_ϵ or A_μ. We find that very similar results are obtained when either A_ϵ or A_μ is chosen but proceed using A_ϵ, as it is possibly appropriate for a larger range of materials (e.g., quadrupolar molecules such as pyrazine). Following Ben-Amotz et al.,[9] we set the centrifugal correction at -0.5 cm^{-1} and take the atmospheric pressure repulsive contribution to be 4.2 cm^{-1}. The Fermi resonance-corrected observed solvent shifts relative to the gas phase for the 23 aprotic solvents are taken and adjusted for these effects to determine, through eq 1, net observed "attractive" solvent shifts $\Delta\nu_A$. The nonspecific contributions to this are then determined by fitting $\Delta\nu_A$ to obtain values for A_ϵ and A_α. Results are shown in Table 3 as fit C and in Figure 1; the RMS error in the fit is 1.9 cm^{-1}, of the order of the uncertainties in the experimental data. The deduced value of A_α is -47.32 cm^{-1}, ca. half of the value of -102 cm^{-1} expected using eq 3 with $\Delta\alpha$ set to our CCSD(T)/cc-pV5Z value of 0.016 Å^3, indicating that this crude equation is only qualitatively descriptive. For each molecule, the deviation between the attractive solvent shift and that obtained from eq 5, fit C, is then taken to be the "observed" specific solvation effect. In Table 4 are shown $\Delta\nu_A$, the fitted nonspecific solvation contributions, and the isolated specific solvent effect. The dispersion term is typically the dominant contribution, but the diversity and extent of the effects of the specific interactions are much wider.

(26) Dunn, W. J., III; Nagy, P. I. *J. Phys. Chem.* **1990**, *94*, 2099.

Table 5. Binding Energies ΔE and CN Frequency Shifts for Various Complexes of ACN with Single Solvent Molecules, Evaluated Using MP2 or B3LYP[a]

	structure		specific solvation/cm^{-1}			$-\Delta E$/kcal mol^{-1} [c]					
						B3LYP			MP2		
solvent	no.	shape	"obs"	B3LYP[b]	MP2	raw	BSSE	+ZPT	raw	BSSE	+ZPT
TFAA		linear	28.4	21.9	29.0	10.3	8.3	7.6	10.2	7.8	6.9
		cyclic		14.7	12.5	10.4	8.0	7.2	10.6	7.1	6.2
HFIP		linear	27.5	20.7		8.4	5.4	4.6			
Li^+ [d]		linear	20	14.3		32.4	29.8	28.8			
TFE		linear	15.4	14.6	17.7	7.5	4.9	4.1	7.9	4.9	4.2
		cyclic (F)		1.5*	9.9	7.7	4.4	3.6	8.1	4.4	3.6
AA		cyclic	12.5	−10.1*	6.7	8.9	6.6	5.7	9.2	5.5	4.5
		con. linear		19.6	20.9	7.0	5.0	4.2	7.1	4.9	4.0
PhOH		linear	[12][e]	13.6	15.0	7.6	5.7	4.8	8.2	5.9	5.0
BzOH		linear	9.8	13.2		6.0	4.1	3.3			
EtOH		linear	7.1	11.8	12.5	5.8	3.8	3.0	6.1	4.0	3.1
HOH	**3**	linear	6.8	9.9	11.8	5.3	3.6	2.3	5.2	3.5	2.3
	4	cyclic		−9.8*	−1.2	5.5	2.9	1.7	5.5	3.1	2.0
		bifurcated		3.1	5.5	4.5	2.3	1.5	4.5	2.5	1.7
	5	reversed			−1.8				3.4	1.5	0.9
		cyc. bifur.		−8.0*	−0.3	6.4	2.0	0.6	6.4	1.9	0.5
PrOH		linear	6.7	8.8	8.3	5.3	3.3	2.4	6.3	3.9	3.0
BuOH		linear	6.4	8.3		5.4	3.3	2.5			
MeOH	**9**	linear	5.3	11.7	12.9	5.8	3.9	3.0	6.0	4.0	3.1
	10	cyclic		−10.7*	−2.8	5.8	2.5	1.4	6.6	2.6	1.5
		cyclic C_s		−10.5*	−1.9	3.9	1.6	1.2	4.3	1.8	1.5
F	**13**	cyclic	3.0	−14.7*	1.2	8.7	5.7	4.3	8.9	5.6	5.4
$CHCl_3$	**11**	linear	2.0	9.6	10.0	4.8	3.4	2.9	5.3	3.7	3.3
	12	cyclic			−0.1				5.1	3.3	2.8
		reverse		−1.2*	−0.9	1.0	0.3	0.1	2.3	1.3	1.1
Py	**15**	cyclic	0.7	−10.5*	−5.6	4.7	2.8	2.0	5.9	3.5	2.8
	16	reversed		−6.2*	−2.7	4.1	2.3	1.6	4.8	2.8	2.1
CCl_4		linear	0.0	0.2	2.9	0.0	−0.6	−0.7	2.5	1.6	1.4
		reversed			−1.9				2.3	0.7	0.3
ACN	**1**	cyclic	−0.5	−7.4*	−1.8	5.1	3.6	2.8	6.4	4.5	3.7
		cyclic TS		−6.9*	−1.5	4.0	2.7	2.3	6.1	4.1	3.5
	2	linear		1.6	3.2	2.7	1.8	1.6	3.1	2.1	1.8
THF	**14**	cyclic	−2.7	−8.9*	−6.3	4.3	1.8	1.0	7.3	3.4	2.5
		cyclic TS			−4.8				6.0	2.4	1.5
Cl^-		reverse (H)	[−8][f]	−39.5*	−13.2	18.1	14.9	14.9	16.3	12.8	12.7
		reverse C_{3v}		−32.5*		16.3	12.1	12.3			

[a] Numbered structures are shown in Figure 2,while all structures are given in the Supporting Information. Calculated gas-phase complex frequency shifts $\Delta\nu$ are, in fact, compared to the "observed" solution-phase specific solvation effect taken from Table 4. [b] An asterisk indicates that B3LYP is inappropriate for evaluating $\Delta\nu$ for this (nonlinear) structure. [c] ΔE is given as the raw energy, that as corrected for basis-set-superposition error (BSSE), and that with both BSSE and zero-point energy correction (ZPT). [d] Calculations for T_d ACN_4Li^+, energies are per ACN, obs is for Li^+ in ACN.[39] [e] Observed value[37,40] for PhOH and ACN doubly dilute in CCl_4. [f] Estimate is that as observed[41] for dilute Br^- in ACN.

b. Properties of Dimeric Solvent−Acetonitrile Complexes. We have considered the properties of gas-phase complexes formed between acetonitrile and one or more of 19 different molecules through ab initio MP2 and B3LYP density functional calculations using Gaussian 94.[27] All calculations were performed using the cc-pVDZ[28] basis set. For each molecule, geometry optimizations were performed searching for stationary points on the potential surface, and these were followed by normal coordinate analyses and zero-point (ZPT) energy and counterpoise basis set superposition error (BSSE) correction. The relative merits of different ab initio and density functional schemes for the evaluation of the properties of intermolecular complexes are outside the scope of this work, but the methods chosen are selected for both their reliability and their feasibility given the size of the complexes considered;[29−38] addition of augmented basis functions to reduce BSSE appears the most obvious possible improvement.[34,36,38] All molecules were considered using B3LYP, but MP2 analyses were not feasible for the largest solutes: HFIP, BzOH, and BuOH. Important results are given in Table 5 and in Figure 2, and all results (95 cluster and 45 monomer geometries, energies, Mulliken charges, and vibrational frequencies, and normal modes) are given in the Supporting Information.

(27) Frisch, M. J.; Trucks, G. W.; Schlegel, H. B.; Gill, P. M. W.; Johnson, B. G.; Robb, M. A.; Cheeseman, J. R.; Kieth, T. A.; Petersson, G. A.; Montgomery, J. A.; Raghavachari, K.; Al-Laham, M. A.; Zakrzewski, V. G.; Ortiz, J. V.; Foresman, J. B.; Cioslowski, J.; Stefanov, B. B.; Nanayakkara, A.; Challacombe, M.; Peng, C. Y.; Ayala, P. A.; Chen, W.; Wong, M. W.; Andres, J. L.; Replogle, E. S.; Gomperts, R.; Martin, R. L.; Fox, D. J.; Binkley, J. S.; DeFrees, D. J.; Baker, J.; Stewart, J. J. P.; Head-Gordon, M.; Gonzalez, C.; Pople, J. A. *Gaussian 94*; Gaussian Inc.: Pittsburgh, PA, 1995.

(28) Woon, D. E.; Dunning, T. H. *J. Chem. Phys.* **1993**, *98*, 1358.

(29) Estrin, D. A.; Paglieri, L.; Corongiu, G.; Clementi, E. J. Phys. Chem. **1996**, *100*, 8701.

(30) Xantheas, S. S. *J. Chem. Phys.* **1995**, *102*, 4505.

(31) Jackowski, K. *Chem. Phys. Lett.* **1992**, *194*, 167.

(32) Mathieu, D.; Defranceschi, M.; Delhalle, J. *Int. J. Quantum Chem.* **1993**, *45*, 735.

(33) Defranceschi, M.; Peeters, D.; Mathieu, D.; Delhalle, J.; Lécayon, G. *Theochem* **1993**, *287*, 153.

(34) Spoliti, M.; Bencivenni, L.; Ramondo, F. *Theochem* **1994**, *1994*, 185.

(35) Stefanovich, E. V.; Thuong, T. N. *J. Chem. Phys.* **1996**, *105*, 2961.

(36) Paizs, B.; Suhai, S. *J. Comput. Chem.* **1998**, *19*, 575.

(37) Melikova, S.; Shchepkin, D.; Koll, A. *J. Mol. Struct.* **1998**, *448*, 239.

(38) Rablen, P. R.; Lockman, J. W.; Jorgensen, W. L. *J. Phys. Chem. A* **1998**, *102*, 3782.

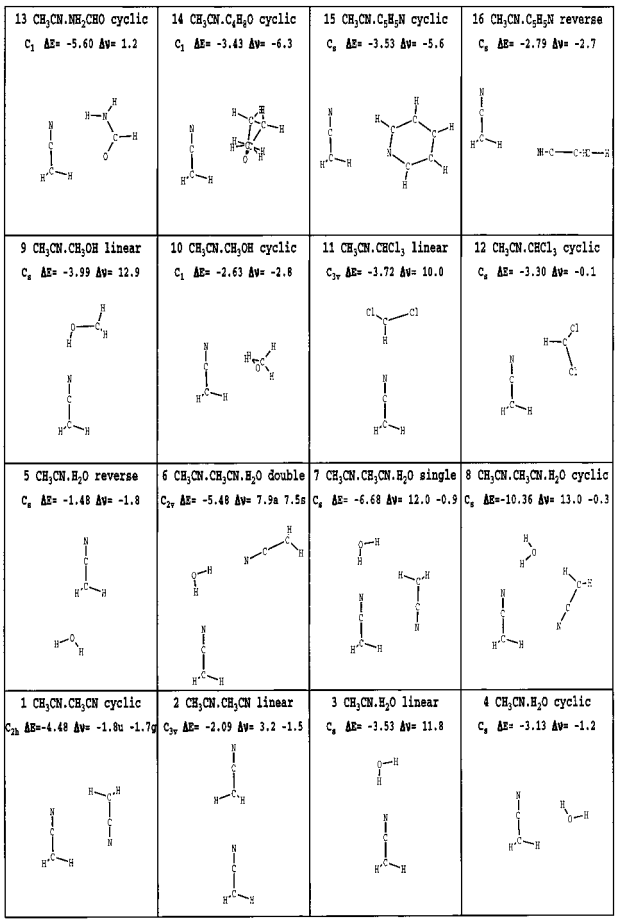

Figure 2. MP2/cc-pVDZ-optimized gas-phase structures for clusters of ACN with ACN, HOH, ACN and HOH, MeOH, $CHCl_3$, F (NH_2-CHO), THF (C_4H_8O), and Py (C_5H_5N). ΔE is the binding energy after BSSE correction, in kcal mol^{-1}, and $\Delta\nu$ is the change in the CN stretch frequency, in cm^{-1}.

In general, the calculated B3LYP and MP2 structures and energetics are very similar. However, the calculated shifts in ν_2 are comparable only for linear hydrogen-bonding configurations. To estimate the errors in our calculated frequency shifts for complexes of this type, we consider solutions of Li^+ dissolved in acetonitrile.[39] The observed CN frequency shift is +20 cm^{-1}, and ACN is found to have a coordination number of 4 around Li^+. B3LYP calculations for tetrahedral $ACN_4{\cdot}Li^+$ predicts frequency changes of 14.3 (allowed T_2) and 15.9 cm^{-1} (forbidden A_1), in reasonable agreement with the observed data. Similar calculations for ACN·Li predict a change of only 2.5 cm^{-1}, however, supporting the original assignment of the solution structure. Also, a second test was performed for ACN·PhOH, which has been observed[37,40] doubly dilute in CCl_4 solution. After correcting the observed frequency[40] of ν_2 = 2262.5 cm^{-1} for nonspecific solvation by CCl_4, an estimated cluster-specific solvation effect of 12 cm^{-1} is obtained, close to the B3LYP- and MP2-calculated values of 13.6 and 15.0 cm^{-1}, respectively.

For nonlinear configurations, however, especially ones for which dispersion interactions are important, B3LYP predicts frequency changes which are up to 25 cm^{-1} more negative, and in section 6 we find that only the MP2 results are consistent with the experimental solvent shift data. Failure of B3LYP to describe this aspect of the problem is not surprising as, for these geometries, dispersive interactions dominate $\Delta\nu$: dispersion is a highly nonlocal correlation effect and as such is not included in current density functional approaches. As a model system we considered the complex ACN·Cl^- (see Table 5), which provides an interesting test case. Unfortunately, $\Delta\nu$ for this complex is not known experimentally, but a shift of ca. −10 cm^{-1} is found[41] for ACN·Br^-, in reasonable agreement with the MP2 results (for ACN·Cl^-) of −13 cm^{-1} but far from the B3LYP result, −40 cm^{-1}. Both MP2 and B3LYP produce excellent values for the binding energy of the chloride, −12.7 and −14.9 kcal mol^{-1}, respectively, compared to the available experimental estimate[42] of −14 to −16 kcal mol^{-1}.

6. Rationalizing the Solvent Shift on the Basis of the Solvent Structure

The structure of a solvent around a chromophore is controlled by the solvent−solute interactions, the solvent−solvent interactions, and the entropy. If the solvent−solute interaction is strong and somewhat directional, as is typically the case when hydrogen bonding is involved, this will be the most influential force, and in the liquid structure will be found solvent molecules tightly bound in configurations closely resembling those adopted by gas-phase clusters. However, if the solvent−solute interaction is either weak or nondirectional, or has a variety of low-energy local minima, then it is the solvent forces which will control the structure. A further complication is that, when solute−solute forces are large, the possibility of solute dimers (or larger species) forming in the solution must be considered. This will have a significant effect on the solvent shift.

a. Liquid Acetonitrile. In the solid phase,[13,43] ACN consists of chains of molecules linked head-to-tail with parallel dipole moments, with each chain surrounded by four antiparallel chains. X-ray and neutron diffraction studies of liquid ACN show qualitatively similar features with an average distance between chains from 3.3[44] to 3.8[45] Å. In the liquid, there is strong short-range order, with 95% occupancy of nearest-neighbor sites reported experimentally,[45] but little order beyond this. Simulations[46,47] successfully reproduce the experimental structure factors, indicate that the nearest-neighbor structure is, itself, quite distorted, and suggest that only three of the four antiparallel nearest neighbors are, on average, present.

The IR and Raman absorption profiles of ν_2 is asymmetric, and there is strong evidence for the existence of a secondary absorption red-shifted by 5 cm^{-1} from the main peak. Initially, this band was assigned by Loewenschuss and Yellin[48] as the acetonitrile dimer, ACN_2, a complex thought to be in equilibrium with uncomplexed ACN in the neat liquid. Later, however, this interpretation of the ν_2 band profile data was challenged by Fini and Mirone,[49] who suggested that the secondary structure is, in fact, a *hot band*. Hot bands appear in a spectrum as the temperature increases but are unaffected by dilution. In this case,

(39) Solovieva, L. A.; Akopyan, S. Kh.; Vilaseca, E. *Spectrochim. Acta* **1994**, *50A*, 683.
(40) Borisenko, V. E.; Koll, A.; Shchepkin, D. N. In *Molecular Spectroscopy, Vol. 3*; Meister, T. G., Ed.; Lenningrad State University: Lenningrad, 1975; p 70.
(41) Jayaraj, A. F.; Singh, S. *J. Mol. Struct.* **1994**, *327*, 107.
(42) Yang, Y.; Linnert, H. V.; Riveros, J. M.; Williams, K. R.; Eyler, J. E. *J. Phys. Chem. A* **1997**, *101*, 2371.
(43) Barrow, M. *Acta Crystallogr. B* **1981**, *37*, 2239.
(44) Radnai, T.; Itoh, S.; Ohtaki, H. *Bull. Chem. Soc. Jpn.* **1988**, *61*, 3845.
(45) Kratochwill, V. A.; Weidner, J. U.; Zimmermann, H. *Ber. Bunsen-Ges. Phys. Chem.* **1973**, *77*, 408.
(46) Bohm, H. J.; Lynden-Bell, R. M.; Madden, P. A.; McDonald, I. R. *Mol. Phys.* **1984**, *51*, 761.
(47) Jorgensen, W. J.; Briggs, J. M. *Mol. Phys.* **1988**, *63*, 547.
(48) Loewenschuss, A.; Yellin, N. *Spectrochim. Acta* **1975**, *31A*, 207.
(49) Fini, G.; Mirone, P. *Spectrochim. Acta* **1976**, *32A*, 439.

Table 6. Calculated (Gas Phase) and Observed[52] (in Ar or CCl_4 Matrix) Intermolecular Vibration Frequencies for the ACN Dimer, in cm^{-1}

	calculated		observed	
symmetry	B3LYP	MP2	Ar	CCl_4
a_g	101	110		111
a_g	80	81	93	
a_u	101	98	159	153
a_u	44	40	105	93
b_g	99	89	76	77
b_u	109	122	124	124

Fini and Mirone postulate that, at room temperature, the ACN vibration ν_8 at[14] 369 cm^{-1} would be slightly populated, and that ν_2 is 5 cm^{-1} lower in frequency when ν_8 is excited compared to when it is not. Indeed, a hot band is observed as a second Q-branch in low-resolution gas-phase spectra of ACN, and the solution band appears insensitive to dilution. Loewenschuss and Yellin later strongly defended[50] their original assignment. Modern works remain divided as to whether the dimerization model is accepted[4,10] or rejected.[7,9]

The spectrum of ACN_2 has been observed[51] in argon matrix at 20 K and the dimerization shift found to be -1.8 cm^{-1}. Strong evidence was found indicating that the dimer has C_{2h} symmetry, indicative of an antiparallel configuration of the monomer units. This cyclic structure, **1** as shown in Figure 2, has been modeled theoretically[31−33] at the SCF and MP2 levels and is predicted to have an interaxis separation of 3.3 Å, consistent with the interchain spacing observed[44,45] in liquid ACN. Our B3LYP and MP2 calculations are in agreement with these results and predict that the cyclic transition state (TS) for rotation about the C−C−N axis affords BSSE-ZPT-corrected energy barriers of just 0.5 and 0.2 kcal mol^{-1}, respectively (see Table 5). Calculated and observed[52] intermolecular vibration frequencies are shown in Table 6, and with perhaps the exception of the two a_u modes (scissors and rollers, see Supporting Information), excellent agreement is found, indicating that the calculations provide adequate descriptions of the local intermolecular potential energy surfaces. There is also a second local minimum, a linear ACN dimer **2** (see Figure 2), ca. 1.5 kcal mol^{-1} higher in energy, which is closely akin to the chain structures found in solid ACN. Hence, we see that the ACN dimer structures correspond to those typically found for nearest-neighbor ACN molecules in the liquid and solid phases. One can conclude from this that either the liquid should be considered as completely dimerized or, to the contrary, no dimers exist at all. Given the floppy nature of the liquid structure suggested by the X-ray[44,45] and simulation[46,47] results, the latter option is preferred, with little real pairing apparent.

If, indeed, a characterizable dimer complex does account for the shoulder at $\nu_2 - 5$ cm^{-1}, then, as the observed[51] argon matrix shift is just -1.8 cm^{-1}, this shift must be highly solvent dependent. Our calculated frequency change at the MP2 level (see Table 5) for the C_{2h} dimer is -1.8 cm^{-1} (see Figure 2 or Table 5), in excellent agreement with the matrix isolation value. Hence, if the shoulder indeed corresponds to a dimer, then the solvent shift of the "dimer" must exceed that of the "monomer" by 3 cm^{-1}.

The dispute between Loewenschuss and Yellin[48,50] and Fini and Mirone[49] concerning the identity of the shoulder revolves around whether the shoulder band is intensified in ACN solutions in hydroxylic solvents: clearly, if the shoulder is a hot band, then its relative intensity would be independent of solvent. In dilute solutions in hydroxylic solvents, ν_2 appears as two poorly resolved bands separated by ca. 5 cm^{-1}, and Fawcett et al.[10] follow the interpretation of Loewenschuss and Yellin and take the lower band to represent solvated ACN dimers, with the upper band corresponding to solvated monomers. However, the lower bands in Fawcett et al.'s spectra clearly themselves show a shoulder 5 cm^{-1} to their red, and it is this shoulder which corresponds to the one observed in pure ACN. Hence, the shoulder is *not* intensified in hydroxylic solvents (this is also seen clearly in the spectra for ACN in HOH shown later in Figure 3). Last, hydrogen bonding to the nitrogen atom of ACN would sterically hinder antiparallel dimer formation. Thus, if the solvated dimer model were valid, the intensity of the dimer peak would *decrease* in hydroxylic solvents rather than increase, as is claimed.

Possible indications that neat acetonitrile has an intrinsic tendency to dimerize come from experimental[53] and theoretical[54−56] studies of the properties of gas-phase clusters ACN_n, with $n = 2-9$. These show solidlike structures at low temperature which, for n odd, have at least one ACN molecule with fewer intermolecular interactions than the rest. At higher temperatures, these clusters melt to form a liquidlike phase. Interestingly, the odd clusters melt at lower temperatures, and the results are interpreted in terms of dimer formation within the clusters. Larger cluster sizes[56] in the range of $n = 10-256$ show little odd−even differentiation, however, although 60% of the ACN molecules have an antiparallel neighbor within 4.5 Å with its dipole oriented to within 30° in what is termed a dimer configuration. Integration of the calculated radial distribution functions (Figure 10b of ref 56) indicates a nearest-neighbor coordination number of 3, however, indicating that many close-by molecules exist but are, on average, poorly aligned. Indeed, these cluster radial distribution functions are very similar to those found[44,45] and simulated[46,47] for liquid ACN. The key question is whether a closely aligned pair should be considered as a dimer, a chemical species existing in its own right. For the liquid, vibrational line broadening is known[57,58] to occur *homogeneously*, indicating that aligned and unaligned neighbors rapidly interconvert without a significant energy barrier. Hence, while oriented dimers may appear in configurational snapshots, they are *not* separate entities within the liquid.

In conclusion, we see that the X-ray, neutron scattering, molecular simulation, matrix isolation, gas-phase cluster, liquid relaxation, ab initio, and spectroscopic evidence is conclusive and indicates that ACN dimers are not present as discernible entities within ACN neat liquid. The "observed" specific solvation effect from Table 5 is -0.5 cm^{-1}, in good agreement with the MP2-calculated value of -1.8 cm^{-1}.

b. Acetonitrile in Water. A notable omission in most studies of the CN solvent shift is acetonitrile in water (HOH), the exception being that of Eaton et al.,[1] who recognized the central importance of this solvent. Unfortunately, they were able to obtain only infrared spectra with insufficient resolution to identify what, using Fourier transform Raman (FT-Raman) spectroscopy, we find to be the key feature. We have taken the spectra of ACN in HOH over the full concentration range at

(50) Loewenschuss, A.; Yellin, N. *Spectrochim. Acta* **1976**, *32A*, 1249.
(51) Freedman, T. B.; Nixon, E. R. *Spectrochim. Acta* **1972**, *28A*, 1375.
(52) Langel, W.; Kollhoff, H.; knözinger, E. *Ber. Bunsen-Ges. Phys. Chem.* **1985**, *89*, 927.
(53) Buck, U. *Ber. Bunsen-Ges. Phys. Chem.* **1992**, *96*, 1275.
(54) Del Mistro, G.; Stace, A. J. *J. Chem. Phys.* **1993**, *99*, 4656.
(55) Stace, A. J.; Del Mistro, G. *J. Chem. Phys.* **1995**, *102*, 5990.
(56) Wright, D.; El-Shall, M. S. *J. Chem. Phys.* **1994**, *100*, 3791.
(57) Schroeder, J.; Schiemann, V. H.; Sharko, P. T.; Jonas, J. *J. Chem. Phys.* **1977**, *66*, 3215.
(58) Berg, M.; Anton, A.; Bout, V. *Acc. Chem. Res.* **1997**, *30*, 65.

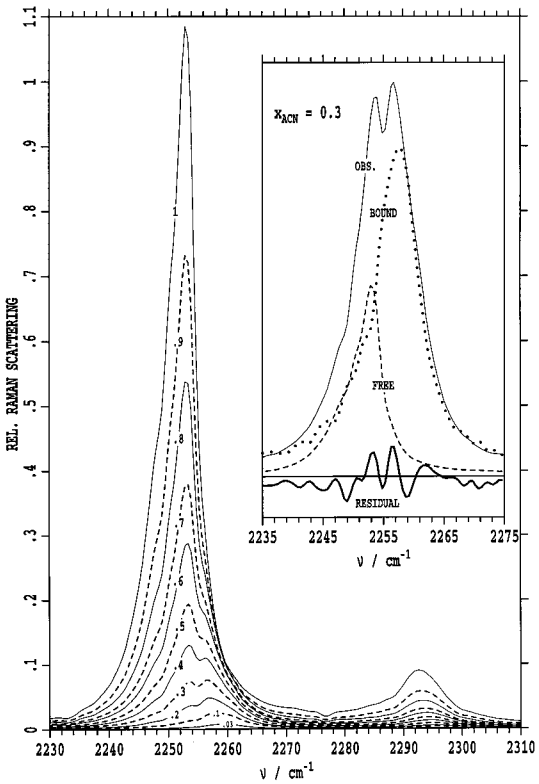

Figure 3. Observed CN Raman scattering intensity as a function of ACN mole fraction x_{ACN} (specified to greater precision in Table 7) in aqueous solution at 295 K. The inset shows the deconvolution of the observed CN stretch band at $x_{ACN} = 0.3$ into two components plus the residual error.

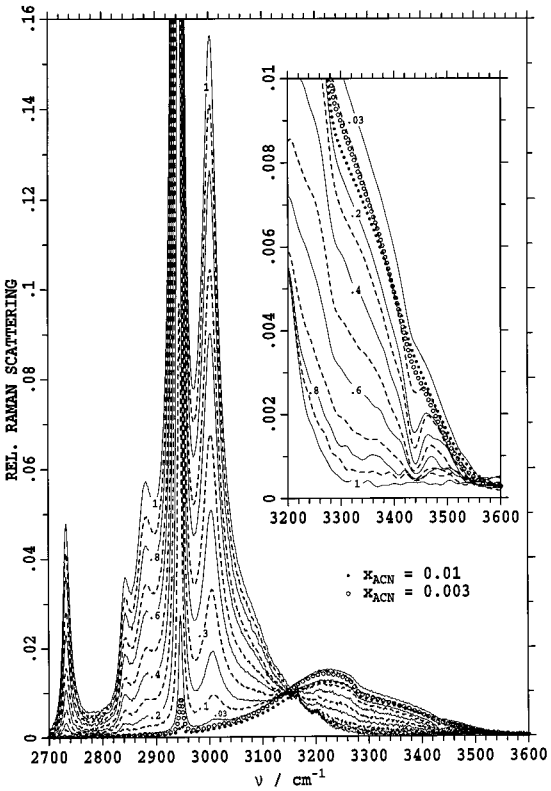

Figure 4. Observed CH and OH Raman scattering intensity as a function of ACN mole fraction x_{ACN} (specified to greater precision in Table 7) in aqueous solution at 295 K. The inset shows the amplified OH region smoothed to a resolution of 3 cm^{-1}.

297 K using a Bruker FT-Raman spectrometer (scan times increased from 1 to 16 h as the ACN mole fraction decreased), and the results are shown in Figures 3 (CN region) and 4 (CH and OH regions). The CN spectra are qualitatively similar to those[10] found in alcohols, with two major bands appearing separated by ca. 5 cm^{-1}, in contrast to the infrared spectra of Eaton et al.,[1] in which only one unresolved band is apparent.

Mixtures of ACN and HOH show a series of unusual properties which can be interpreted in terms of *microheterogeneity*.[2,59] The literature of this field, as well as the variety of experimental information available for ACN−HOH mixtures, has recently been summarized.[3,4,60] Both liquids are miscible and colorless but, within an ACN mole fraction range between 0.15∼0.3 and 0.7, are postulated to separate into discrete regions of liquid acetonitrile and liquid water. Estimates for the shape, size, or interconnectivity of these regions are rare, however, with the most tangible description coming from the simulations of Kovacs and Laaksonen.[3] Similarly, in aqueous solutions at the air/water interface, ACN is known[5] to form a surface layer, the interface structure undergoing a phase transition at an ACN mole fraction of 0.07.

In the bulk for low ACN concentrations, the standard lore[4] is that ACN molecules are separated from each other and fit into "cavities" in the water structure.[61] In a strict sense, this water cavity model is not borne out by computer simulations,[3,24,26] however, which predict that, on average, either 1 or 1.3−1.4 water molecules actually hydrogen bond to the ACN nitrogen (most experimental interpretations suggest that ACN is monohydrated but others do suggest dihydration[1]). The simulations[26] also predict that 19 waters form the first coordination shell: in a water cavity, the coordination number would be nominally 4, 6 at the most. Rather than the ACN molecules fitting into water cavities, it is clear that any single ACN molecule must be surrounded by water. The notation used, however, refers[62] back to old unphysical models[63] for water in which the liquid is thought to exist in a continuous hydrogen-bonded network containing uncoordinated water molecules located in "cavities" in the liquid. Moving on, microheterogeneity is believed to occur in the intermediate concentration region, with its effects enhanced at low temperature, leading eventually to macroscopic phase separation.[64] At high ACN concentrations, the aqueous phase is believed to dissolve within the ACN phase, producing isolated HOH molecules hydrogen bonded to ACN.

Qualitatively, our observed spectra of ν_2 for ACN in water shown in Figure 3 are readily interpreted in terms of microheterogeneity. At high ACN concentration, one peak appears in the spectrum at 2253.2 cm^{-1}, with the Fermi resonance-enhanced mode $\nu_3 + \nu_4$ appearing at 2292.3 cm^{-1} and the shoulder due to the ν_8 hot band discernible (over the whole concentration range) at ca. 2248 cm^{-1}. These bands remain in place as the ACN concentration falls, but a new blue-shifted band appears, becoming stronger and moving to higher frequency as the ACN concentration continues to fall. Eaton et al.[1] have also shown that the frequency shift increases significantly with decreasing temperature, but they did not resolve

(59) Naberukhin, Y. I.; Rogov, V. A. *Russ. Chem. Rev.* **1971**, *40*, 207.
(60) Blandamer, M. J.; Blundell, N. J.; Burgress, J.; Cowless, H. J.; Horn, I. M. *J. Chem. Soc., Faraday Trans.* **1990**, *86*, 277.
(61) Dack, M. R. J. *Aust. J. Chem.* **1976**, *29*, 771.
(62) Balakrishnan, S.; Easteal, A. J. *Aust. J. Chem.* **1981**, *34*, 943.
(63) Frank, H. S.; Quist, A. S. *J. Chem. Phys.* **1961**, *34*, 604.
(64) Armitage, D. A.; Blandamer, M. J.; Foster, M. J.; Hidden, N. J.; Morcom, K. W.; Symons, M. C. R.; Wotton, W. J. *Trans. Faraday Soc.* **1968**, *64*, 1193.

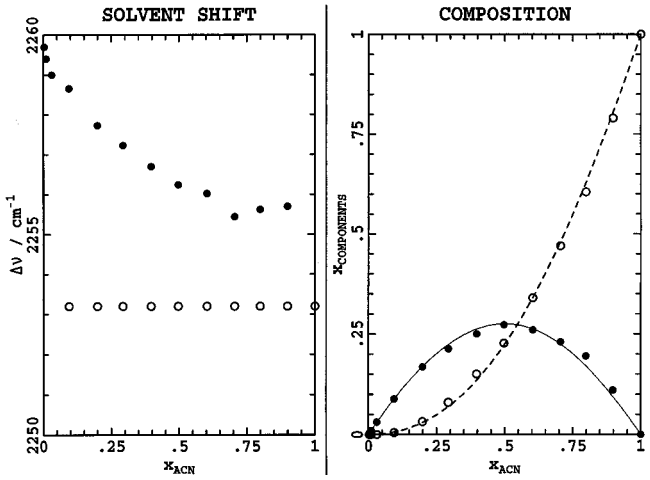

Figure 5. For the bound and free ACN components extracted from the Raman scattering of ACN in aqueous solution is shown the frequency of its band maximum and the mole fraction of ACN in each component. ○, free ACN; ●, bound ACN.

Table 7. The Frequency, in cm^{-1}, of the Band Centers of the Bound and Free Components of ACN in HOH as a Function of x_{ACN}, the Mole Fraction of ACN (for Clarity, Reduced Precision Is Used in Text and Figures), and the Mole Fraction of ACN Attributed to Each Component

	bound ACN		free ACN	
x_{ACN}	ν	x	ν	x
0.0029	2259.7	0.0029		0.000
0.0098	2259.4	0.0098		0.000
0.031	2259.0	0.031		0.000
0.095	2258.7	0.089	2253.2	0.006
0.199	2257.7	0.168	2253.2	0.032
0.293	2257.2	0.213	2253.2	0.077
0.397	2256.7	0.250	2253.2	0.150
0.497	2256.2	0.273	2253.2	0.227
0.603	2256.0	0.260	2253.2	0.340
0.705	2255.4	0.230	2253.2	0.470
0.799	2255.6	0.195	2253.2	0.605
0.899	2255.7	0.110	2253.2	0.790
1		0	2253.2	1

the CN band into two peaks. The original peak is attributed to regions of "free" or "liquid" ACN, while the blue-shifted peak is attributed to "bound" ACN molecules, ones which have a CN−HOH hydrogen bond.

Quantitatively, assuming that the Raman intensity is proportional to mole fraction, we have deconvolved the observed band profile into two bands, and the deduced center and intensity of each of the two components are given as functions of ACN mole fraction in Figure 5 and Table 7. To complete this deconvolution, we fitted the observed total intensity to the shifted and scaled sums of bands of fixed profile, the $x_{ACN} = 1$ and $x_{ACN} = 0.0098$ profiles chosen to represent the low-frequency and high-frequency components, respectively. This simple procedure proved to be appropriate, and a sample deconvolution with its associated residual error is shown in Figure 3 for $x_{ACN} = 0.3$. The results indicate that the band attributed to free ACN remains at precisely the same frequency, that found for neat ACN liquid. Based on the microheterogeneity model, this is the result expected if ACN is present in nanoscopic domains. Further, this band disappears at ca. 10% ACN mole fraction, a value consistent with other estimates[3,4,59] for the onset of microheterogeneity. For the hydrogen-bonded band, a spectral shift is found which moves progressively further to the blue as the concentration is lowered, possibly reflecting a steadily increasing degree of aquation. Evidence supporting this can be found from ab initio calculations of the properties of the ACN−HOH complex, see Table 5 and Figure 2. The lowest energy complex, **3** (see also refs 38, 65, and 66), has a linear hydrogen-bonded structure and is calculated to produce a shift of 11.8 cm^{-1} using MP2 (9.9 cm^{-1} using B3LYP), more than the "observed" specific solvent shift of 6.8 cm^{-1}. However, there exists[65,66] a cyclic non-hydrogen-bonded structure, **4,** at a MP2 BSSE+ZPT-corrected energy 0.3 kcal mol^{-1} higher, for which the shift of ν_2 is very different, -1.2 cm^{-1}. In solution, if an ACN molecule is near another in an antiparallel structure like **1**, then direct access of a water molecule to form a linear hydrogen bond is sterically hindered (see, e.g., structures **7** and **8** in Figure 2). As the hydrogen bond is only weakly angularly dependent, it is thus quite likely that the optimal linear hydrogen bond is not formed in the solution but rather a distorted hydrogen bond with the water molecule moved to one side. Such displacement is likely to have a profound effect in reducing $\Delta\nu$, however. Hence, it is not suprizing that the solvent shift increases significantly as the ratio of water molecules to ACN molecules neighboring an ACN molecule increases. This effect can also account for the significant increase in the solvent shift found for dilute ACN in HOH and MeOH as the temperature decreases.[1]

The observed mole fractions of bound and free ACN may be rationalized using the scheme

$$\text{ACN}-\text{ACN} + \text{HOH}-\text{HOH} \overset{K'}{\rightleftharpoons} 2\text{ACN}-\text{HOH} \qquad (8)$$

This reaction should be interpreted as the breaking of one ACN-to-ACN interaction plus one water-to-water hydrogen bond and the formation of two ACN-to-water hydrogen bonds, with other associations or hydrogen bonds involving the molecules concerned remaining intact:

$$K' = \frac{[\text{concn of ACN}-\text{HOH bonds}]^2}{[\text{concn of ACN}-\text{ACN bonds}][\text{concn of HOH}-\text{HOH bonds}]} \qquad (9)$$

or, assuming two hydrogen bonds per liquid water molecule and the experimental result (given 95% nearest-neighbor occupancy[45]) of two nearest-neighbor interactions per liquid ACN molecule,

$$K = \frac{K'}{4} = \frac{x_{\text{ACN}_{\text{bound}}}{}^2}{x_{\text{ACN}_{\text{free}}} x_{\text{HOH}_{\text{free}}}} \qquad (10)$$

where the x's are the respective component mole fractions. We stress that "free" means not hydrogen bonded to the other species. At total ACN mole fraction x_{ACN}, this gives

(65) Damewood, J. R., Jr.; Kumpf, R. A. *J. Phys. Chem.* **1987**, *91*, 3449.
(66) Sathyan, N.; Santhanam, V.; Sobhanadri, J. *Theochem* **1995**, *333*, 179.
(67) McTigue, P.; Renowden, P. V. *J. Chem. Soc., Faraday Trans. 1* **1975**, 1784.
(68) Sivakumar, T. C.; Rice, S. A.; Sceats, M. G. *J. Chem. Phys.* **1978**, *69*, 3468.
(69) Coker, D. F.; Miller, R. E.; Watts, R. O. *J. Chem. Phys.* **1985**, *82*, 3554.
(70) Lorimer, J. W.; Jones, D. E. *Can. J. Chem.* **1977**, *55*, 2980.
(71) Symons, M. C. R.; Harvey, J. M.; Jackson, S. E. *J. Chem. Soc., Faraday Trans. 1* **1980**, *76*, 256.

$K \neq 1$:

$$x_{\mathrm{ACN_{bound}}} = \frac{K - [K^2 - 4K(K-1)(x_{\mathrm{ACN}} - x_{\mathrm{ACN}}{}^2)]^{1/2}}{2(K-1)}$$

$$x_{\mathrm{ACN_{free}}} = x_{\mathrm{ACN}} - x_{\mathrm{ACN_{bound}}}, \quad x_{\mathrm{HOH_{free}}} = 1 - x_{\mathrm{ACN}} - x_{\mathrm{ACN_{bound}}}$$

$K = 1$: (11)

$$x_{\mathrm{ACN_{bound}}} = x_{\mathrm{ACN}} - x_{\mathrm{ACN}}{}^2, \quad x_{\mathrm{ACN_{free}}} = x_{\mathrm{ACN}}{}^2$$

$$x_{\mathrm{HOH_{free}}} = (1 - x_{\mathrm{ACN}})^2$$

By fitting these equations to the observed data, a value of $K = 1.5$ is obtained, and these predicted bound and free ACN mole fractions are also shown in Figure 5. The agreement between the calculated and experimental data is quite good. It suggests that no distinct point exists at which the onset of microheterogeneity starts, but rather that the observed onset at $x_{\mathrm{ACN}} = 0.1$ corresponds simply to the limit of detectability of the FT-Raman technique for "free" ACN. This result is in contrast to the sharp discontinuity in surface composition found[5] to occur at the air/solution interface at $x_{\mathrm{ACN}} = 0.07$. Also, the properties of dilute ACN in HOH and those of dilute HOH in ACN appear quite similar, contrary to current microheterogeneity descriptions.[3,4,59]

Embodied in eq 11 is a 1:1 molar ratio of ACN to HOH in the bound region. This could occur if ACN accepted at most one hydrogen bond and each water donated at most one hydrogen bond to ACN. However, an alternative interpretation is that ACN forms up to two hydrogen bonds to water with a corresponding increase in water's donation to ACN. Such variation could explain the observed change in $\Delta\nu$ for the bound band with concentration as, at low concentration, one direct linear hydrogen bond could form to CN, while as the concentration increases, two distorted hydrogen bonds form instead. However, the simplicity of the mechanism scheme found to reproduce the experimental component mole fractions renders this interpretation unlikely, as the additional equilibrium constants would need to be very similar to K and the change in tendency of ACN to accept two hydrogen bonds would need be linked to the change in tendency of the water to donate two. This remains a significant but unresolved issue,[1] although most experimental interpretations perceive ACN as only monobasic; indeed, doubly dilute in CCH_4 solution, no evidence for ACN·HOH·ACN has been found.[67] Simulations[3,26] of dilute ACN in HOH have resulted in a variety of predictions ranging from 1 (dimerization allowed[3]) to 1.3−1.4 (no dimerization[26]) to 2 (no dimerization[24]) hydrogen bonds to CN.

Experimental evidence supporting the monobasic nature of ACN can be found in the observed OH region Raman spectra for dilute HOH in ACN shown in Figure 4. Raman spectra in the OH region of water are difficult to interpret[25] as the Raman intensity is very sensitive to molecular environment, preferentially selecting symmetric long-range cooperative motions[68] at the expense of the (high-frequency) majority of the OH vibrational density of states. Nevertheless, an isobestic point is observed at 3150 cm^{-1}, suggesting that no significant change in the CH and allowed OH environments occurs over the whole concentration range, although from Figure 4 it is clear that the intensity of the CH stretch modes varies nonlinearly with concentration. Shown magnified in the inset is the high-frequency tail of the OH band, in which two broad bands near 3360 and 3460 cm^{-1} are seen to grow in as the concentration of HOH in ACN increases. The simplest interpretation of the upper band is that it arises from HOH bound to ACN: the observed[67] value for the OH stretch in the 1:1 complex doubly dilute in CCl_4 is 3555 cm^{-1}, this value being expected[67] to fall significantly if the water is also hydrogen bonded to other waters. If ACN is monobasic, then even at very low water concentration, water−water hydrogen bonds would be expected. Water dimer is known to absorb at 3552 cm^{-1} in CCl_4 solution and at 3532 cm^{-1} in the gas phase,[69] but water trimer absorbs at 3357 and 3400 cm^{-1} in the gas phase,[69] and hence the lower band near 3360 cm^{-1} could thus be interpreted in terms of water clustering. As the water concentration increases, so does the intensity of the main broad liquid water peak centered at 3220 cm^{-1}.

A curious feature of Figure 4 is that the strength of the OH Raman signal increases significantly as ACN is added to liquid water, going through a maximum at around $x_{\mathrm{ACN}} = 0.03$. This suggests that adding ACN to liquid water increases the long-range order of the liquid and hence also increases the Raman vibrational polarizability derivatives. ACN would thus be thought of as a "structure maker". While early reports[70] categorized ACN as a structure breaker, the weight of evidence[1,3,62] does, indeed, characterize ACN as a structure maker.

To aid in the understanding of ACN−HOH mixtures, calculations for additional ACN·HOH and ACN·ACN·HOH clusters have been performed. All results are given in the Supporting Information, but the most interesting structures are also shown in Figure 2. For ACN·HOH, **5** is "reversed", with an interaction between water oxygen and ACN hydrogen. The potential surface describing these interactions appears reasonably flat, **5** being a transition state linking cyclic isomers. Compared to the linear and cyclic isomers, reversed structures have much less binding but yet are sufficient to possibly scavenge non-hydrogen-bonded water oxygens in solution.[71] Structures **6**−**8** are some of the many possible ones for water interacting with two ACN molecules, with **6** representing double linear hydrogen bonding to the water. It is clear that this structure would not easily fit into dilute solution of HOH in ACN as the ACN molecules are roughly perpendicular, not parallel or antiparallel. Also, its energy is 1.6 kcal mol^{-1} less than that for two separated ACN−HOH linear hydrogen bonds, and so the many-body polarization effect is to destabilize the hydrogen bonding, in contrast to HOH−HOH hydrogen bonding, for which many-body effects increase the hydrogen bond strengths. This explains why each water appears to form only one hydrogen bond to ACN, leaving one proton to bind to HOH. Structures **7** and **8** add a water to a cyclic ACN dimer with the oxygen facing away from or into the center, respectively. The simple structure **7** is 1.3 kcal mol^{-1} less stable than the sum of isolated ACN−ACN and ACN−HOH interactions, presumably due to close inter-hydrogen distances. By far, the most stable structure is **8,** which is cyclic and contains linear ACH·HOH, reversed ACN·HOH, and cyclic ACN·ACN contributions, the binding energy being 1.1 kcal mol^{-1} less stable than the sum of the three individual contributions. This is a very floppy structure (see Supporting Information), with nominally a small excluded volume in the middle, but one which could fit into that of liquid ACN.

In terms of the microheterogeneity model in which discrete regions of ACN, HOH, and their interface are expected in solution, the simplicity of eq 11 places serious constraints on the interface topology. For example, in the 1:1 molar liquid, about half of the waters and half of the ACNs are "free", while the other half, those at the "interface", are "bound". Hence, micelle type structures are not permitted. A reasonable topology would be one extended from structures such as **8**, in which ACN and HOH form two independent continuously connected

networks, allowing half of the volume of the system to be considered as the "interface". Moving away from the 1:1 mixture would then simply see swelling in one of the networks and shrinking in the other. Further, while microheterogeneity models postulate three separate chemical regimes (single-phase ACN solvated by liquid HOH, two-phase, and single-phase HOH solvated by liquid ACN) with distinct boundaries, eq 11 sees one continuously evolving chemical system as a function of concentration: microheterogeneity is always present.

In terms of the development of a detailed microscopic model for microheterogeneity, the most significant contribution is the simulations of Kovacs and Laaksonen.[3] They simulated solutions of 0, 0.12, 0.5, 0.8, and 1 mole fraction x_{ACN} of ACN in HOH. Although coarsely grained, their results indicate no major phase changes in the nature of the solution as a function of x_{ACN} but rather steady continuous evolution of structural and dynamical properties. At $x_{ACN} = 0.88$, the water molecules form clusters or chains of water molecules interlocked by hydrogen bonds, with most waters offering also a hydrogen bond to the ACN solvent. Little perturbation to the ACN−ACN radial distribution functions is apparent at this concentration, except for the reduction of head-to-tail correlation. At $x_{ACN} = 0.12$, structure-making effects are seen for the water, but significant ACN−ACN correlation remains, with the nearest-neighbor coordination number reduced from 3 in pure ACN to 1 in dilute solution. These results are consistent with the observed Raman spectra and the calculated MP2 and B3LYP cluster energetics.

c. Acetonitrile in Other Protic Solvents. The solvent shift of ν_2 has been measured in various alcohols and carboxylic acids (see Table 1), and extensive studies have been performed on acetonitrile−methanol mixtures (see, e.g., refs 7, 8, 24, 66, 72, and 73). For MeOH, EtOH, PrOH, BuOH, and AA, Fawcett et al.[10] resolve the main band into two poorly resolved components separated by ca. 5 cm^{-1}, analogous to the bands found in HOH. As discussed earlier, Fawcett et al. incorrectly interpret these bands as arising from hydrogen-bonded ACN monomers and dimers. In the ACN−MeOH literature,[7,8,72] however, the lower band is not attributed to hydrogen-bonded ACN dimers but rather to free ACN molecules, an interpretation which is consistent with our interpretation of the spectra of ACN−HOH mixtures. Simulations of the liquid structure[24] support this analysis.

A remarkable feature of the observed spectra in the systems in which the free ACN band is observed (HOH, MeOH, EtOH, PrOH, BuOH, AA) is that its frequency varies as a function of solvent by less than 0.5 cm^{-1}, a value less than the experimental error in the measurements. Hence, if this corresponds to the vibration of "free" ACN, either the vibration frequency must be extremely *insensitive* to molecular environment and/or the environment is the same *independent* of solvent. Extreme insensitivity to solvent is, however, difficult to envisage, as the dielectric properties of the solvents differ considerably and our calculated MP2 solvent shifts shown in Table 5 are very sensitive to geometry. These calculations, like those for ACN·HOH, predict global minimum structures[66] with linear hydrogen bonds, such as **9,** with large solvent shifts and higher-energy nonlinear structures, such as **10,** with minimal solvent shift. Hence, if the ACN is accessible to the solvent, there must be a range of environments, although considerable averaging could occur due to the presence of several simultaneous solvent−solute interactions, and due to motional narrowing. The alternative option, that the environment around a "free" ACN molecule is independent of solvent, leads again to the concept of microheterogeneity: the "free" ACN collects to form nanoscopic domains of ACN within the solution. Indeed, microheterogeneity is perhaps an apt interpretation of the conclusions of Besnard et al.,[7] that at $x_{ACN} = 0.001$ in MeOH, 20% of the ACN is uncomplexed. Further, at the other extreme of very low concentrations of MeOH in ACN, they found[7,8] that MeOH exists largely as tetramers, a result consistent with microheterogeneity. But if the microheterogeneous domains are as small as this, then, as reasoned for ACN in HOH, the interface region must be large, and so the environments of the free ACN molecules must be variable. Hence, it seems that, to some extent, aspects of both the solvent insensitivity and solvent independence models must apply. Strong evidence supporting this conclusion comes also from studies of electrolytes dissolved in ACN, in which both "free" and "cation-bound" ACN molecules are similarly identified.[39,74]

Only the higher "bound" ν_2 band is seen for BzOH and TFAA (and also TFE and HFIP), an observation which Fawcett et al. attribute to increased hydrogen bond strength. Our B3LYP- and MP2-calculated binding energies, shown in Table 5, show that, while this is a factor, the situation is, in fact, quite complex. For instance, BzOH forms complexes only ca. 1 kcal mol^{-1} more stable than do the other non-fluorinated alcohols, but the bond strength of ACN·AA exceeds that of all other protic solvents except for the TFAA complex. Also, while the effect of fluorination appears larger for AA than for EtOH and PrOH, the calculated smaller change in ΔE arises due to internal hydrogen bonding in TFE and HFIP.[75] While the cyclic isomer (F interacting with CH) retains aspects of this internal hydrogen bonding, the linear isomer does not, and hence it is significantly destabilized. Clearly, the equilibrium between these structures in solution must be quite complex.

Two TFAA·HOH complexes were found, both strongly bound, the most stable one having a linear structure and producing a very large solvent shift, in agreement with the experimental value, and the other having a cyclic (C═O interacting with CH) structure and a more modest solvent shift. Unlike the other protic complexes, for AA·HOH, *only* cyclic (C═O interacting with CH) local minima are found, and the solvent shift reported in Table 5 for a linear configuration is actually obtained by externally constraining the CNH angle at 180°. The AA−ACN interaction is very strong, but it is poorly directional, the observed solvent shift being intermediate between the two calculated values but much closer to that calculated for the cyclic structure. An explanation of the observed presence of both free and bound ACN in AA solution, while only bound ACN is found in TFAA solution, can be found in these geometrical differences, the ca. 2 kcal mol^{-1} additional binding strength for TFAA.ACN, and the relative weakness of the TFAA dimer. Analogous B3LYP and MP2 calculations for AA_2 and $TFAA_2$ (see Supporting Information) predict BSSE-corrected binding energies of −12.0 and −15.2 kcal mol^{-1} for AA_2 (the observed[76] value is −16 kcal mol^{-1}) but only −11.5 and −14.6 kcal mol^{-1} for $TFAA_2$, respectively.

d. Acetonitrile in Carbon Tetrachloride and Chloroform. While our previous calculations have shown that the observed specific interaction can, through knowledge of the liquid structure, be correlated with shifts predicted for solvent−solute complexes when large interactions with protic solvents are involved, $CHCl_3$ and CCl_4 are considered as a type of "control"

(72) Suhai, S. *Int. J. Quantum Chem.* **1992**, *42*, 193.
(73) Yarwood, J. *Chem. Phys. Lett.* **1992**, *208*, 557.
(74) Sadlej, J. *Spectrochim. Acta* **1979**, *35A*, 681.
(75) Purohit, H. D.; Sharma, H. S.; Vyas, A. D. *Bull. Chem. Soc. Jpn.* **1974**, *48*, 327.
(76) Karle, J.; Brockway, L. O. *J. Am. Chem. Soc.* **1944**, *66*, 574.

experiment: the aim is to show that, when no specific interactions are involved, no specific solvent shift is predicted. For CCl_4, the desired result is readily established, with, as shown in Table 5, little binding and no solvent shift. The problem is not quite that straightforward, however, as ACN is known[77] to dimerize in dilute CCl_4 and cyclohexane solutions, but, as we have already argued, such dimerization is also predicted to have minimal effects on the solvent shift.

Of all 18 partners for which we have carried out quantum calculations, reconciliation of the calculated dimer properties and observed solvent shift proved most difficult for $CHCl_3$. As shown in Table 5, both B3LYP and MP2 (and SCF[78]) calculations predict the presence of a strong hydrogen bond type interaction between ACN and the hydrogen from $CHCl_3$ (see structure **11** of Figure 2). The BSSE-corrected bond strength is 3.4−3.8 kcal mol^{-1}, the same as that predicted for the ACN−HOH complex. This runs contrary to chemical intuition, in that $CHCl_3$ is either known as a weak hydrogen bond donor or just simply taken to be a noncomplexing solvent;[10,79] its complexing ability is similar[80] to that of CCl_4. Further, the predicted solvent shift for the hydrogen-bonded complex is ca. 10 cm^{-1}, also comparable to that predicted for HOH, while the observed specific solvation effect of 0.0 cm^{-1} is precisely what is expected for a noninteracting solvent. Raman line shape studies[81] indicate that, in solution, ACN and $CHCl_3$ do interact strongly, but linear hydrogen-bonded complexes are *not* prevalent.

Nevertheless, we believe that it is possible to rationalize the calculated and experimental results. $CHCl_3$ has the highest acceptor number, 23.1, attributable to CH functionality, listed in the standard tables of Gutmann; this value is just slightly less than that for the alcohol BuOH, 27. Also, $CHCl_3$ has a sizable dipole moment, (MP2, B3LYP, and observed values are 1.14, 1.15, and 1.0 D, respectively) and hence it is capable of significant intermolecular interaction. We find that, like the alcohols, the ACN−$CHCl_3$ complex has a second bent local minimum, **12,** for which the predicted solvent shift is 2.2 cm^{-1}. This structure is just 0.2 kcal mol^{-1} higher than the linear one, connected via a transition state at ca. 0.1 kcal mol^{-1} higher energy; after BSSE correction, the linear structure becomes 0.4 kcal mol^{-1} more stable, however. Hence, we see that hydrogen bonding involving $CHCl_3$ is weak not because the bond energy is low but rather because the interaction is poorly directional. It will thus be the solution structure which determines the solvent shift. In the liquid structure[43] of $CHCl_3$, it is known that the first nearest-neighbor molecules align with parallel dipoles, a CH bond pointing between two chlorines of a neighboring molecule. ACN has a molecular volume similar to that of $CHCl_3$ but is prolate rather than oblate. Naively, ACN would be expected to cause the least disturbance to the structure of the $CHCl_3$ if it just replaced one solvent molecule, its long axis aligned parallel to one of the long axes of the replaced molecule. This would generate liquid structures such as **12** and hence not show specific solvation effects, as observed. Indeed, the presence of such structures is implied from the mixed-liquid simulations of Kovacs, Kowalewski, and Laaksonen.[79] Even though their deduced N−H bond length of 2.8 Å is much longer than the value of 2.2 Å optimized for both structures **11** and **12**, the C (from CN)-to-C (from $CHCl_3$) radial distributions show a main peak attributable to **12** but only a weak shoulder attributable to **11**.

e. Acetonitrile in Formamide, Pyridine, and Tetrahydrofuran. These three aprotic solvents all may act as electron donors. They are selected for study, among the aprotic solvents, as formamide (F) is "observed" to have one of the largest positive specific solvent interactions, tetrahydrofuran (THF) to have one of the largest negative interactions, and pyridine (Py), the strongest base after hexamethylphosphoramide (HMPA), to have almost no specific interaction.

For ACN·F, the cyclic structure **13** is found, in which a formamide hydrogen interacts with the CN π system while the oxygen interacts with a methyl hydrogen. Both molecules contain groups which are good electron donors and groups which are poor electron acceptors, and it appears that the formamide hydrogen-to-CN π interaction is the strongest. The resultant shift of ν_2 of 1.6 cm^{-1} is close to the "observed" value, 3.0 cm^{-1}. For ACN·DMF, the structure of the 1:1 molar liquid is known[44] and, like **13**, has an antiparallel arrangement of the ACN and solvent molecular dipoles and has a similar intermolecular spacing. Replacement of H with CH_3 has the effect of rotating the DMF molecule by 90° about its dipole, however, and the nearest-neighbor ACN molecules sit above and below the plane of the DMF.

A thorough scan of the potential surface for ACN·THF was performed, but **14** was the only local minimum found. It is reminiscent of ACN·F in that the structure is cyclic, with THF acting as both an electron donor and acceptor, but this time the oxygen-to-methyl hydrogen interaction is the strongest. The predicted solvent shift is −4.8 cm^{-1}, slightly in excess of the observed value of −2.7 cm^{-1}.

For ACN·Py, optimizations were constrained to C_s symmetry, and two structures were found. The lowest energy structure, **15**, is reminiscent of **13** and **14**, although the only significant interaction is the nitrogen-to-methyl hydrogen interaction. From this, a large specific solvation effect of −5.6 cm^{-1} is calculated, in contrast to the "observed" specific solvation of +0.7 cm^{-1}. Naively, however, a large negative effect of this magnitude was expected as pyridine is a strong base. The other structure, **16**, is predicted to be 0.7 kcal mol^{-1} higher in energy, although this difference may be somewhat inflated as this C_s-constrained structure is, in fact, a transition state. For it, the calculated frequency shift is just −2.7 cm^{-1}, much nearer the "observed" value. Hence, it appears that the details of the solution structure are also critical for this system. π-stacking interactions are also possible.[82] Another issue that may be relevant here is that we have implicitly assumed that the solvent molecule involved in a specific interaction has no volume during the prior evaluation of the dispersion contribution to the solvent shift. This is clearly a poor approximation for pyridine, and it could be that a significant part of the specific interaction is dispersive in origin, and hence this contribution is double-counted.

In the above discussions, we have considered only the possibility of specific interactions occurring between ACN and a single base molecule whereas, in principle, simultaneous interactions with up to three base molecules are possible—this is the "double counting" problem described in section 5. Such multiple interactions would put significant constraints on the liquid structure, however. Also, if multiple bonding occurs, then a significant large fraction of the volume around the solute would be comprised of these molecules, and hence, to avoid

(77) Saitô, H.; Tanaka, Y.; Nagata, S.; Nukada, K. *Can. J. Chem.* **1973**, *51*, 2118.

(78) Figeys, H. P.; Geerlings, P.; Berckmans, D.; Van Alsenoy, C. *J. Chem. Soc., Faraday Trans. 2* **1981**, *77*, 721.

(79) Kovacs, H.; Kowalewski, J.; Laaksonen, A. *J. Phys. Chem.* **1990**, *94*, 7378.

(80) Fenby, D. J.; Chand, A.; Inglese, A.; Grolier, J.-P. E.; Kehiaian, H. V. *Aust. J. Chem.* **1977**, *30*, 1401.

(81) Moradi-Araghi, A.; Schwartz, M. *J. Chem. Phys.* **1978**, *68*, 5548.

(82) Aroney, M. J.; Patsalides, E.; Pierens, R. K. *Aust. J. Chem.* **1985**, *38*, 507.

double counting, their contributions would have also been included in the nonspecific solvation terms. Formamide, being small and strongly interacting, is the most likely candidate for multiple bonding.

7. Conclusions

Research on the solvation of acetonitrile has progressed in different, often uncorrelated, directions. We have shown that it is possible to formulate a general description of this solvation which, in principle, includes and correlates all known aspects. This picture, however, is a complex one in which physical properties of acetonitrile solutions, such as the solvent shift $\Delta\nu$, arise from fundamental intermolecular interactions convolved (homogeneously or inhomogeneously) with the structure of the solution. Indeed, much of this complexity arises by way of the solution structure itself. Acetonitrile is a very important solvent, and one of the key reasons for this is that it contains a hydrophobic methyl group connected to a hydrophilic cyano group and can thus be thought of as an extremely small surfactant. It is then not so surprising that macromolecular structures, as postulated in solvent microheterogeneity theories, can arise. It seems apparent that the thermodynamic data[3,4] which led to ideas of microheterogeneity are describing the same physical effects that give rise to $\Delta\nu$ for acetonitrile in water *and* the weaker alcohols[7,8] and in electrolyte solutions,[39,74] as well as possibly other solvents. When solvent interactions are very strong and directional, as found for the fluorinated solvents, these tend to dominate the structure of the solvent around acetonitrile, and solvation properties are easily understood. However, for weaker solvent−solute interactions, such as those for water, the weaker alcohols, chloroform, and pyridine, other factors will contribute to or even completely determine the structure.

Of all the systems which we consider, two paradigm comparisons can be found. These are comparison of (i) ACN in HOH or $CHCl_3$ and (ii) ACN in AA or TFAA. The complexes ACN·HOH and ACN·$CHCl_3$ appear very similar, both having linear structures of similar energy producing similar solvent shifts, both having also cyclic structures slightly higher in energy producing minimal solvent shifts. Yet, for ACN in HOH, a moderately large specific solvent shift is observed, while only a small shift is seen for ACN in $CHCl_3$: in these systems, it is the solvent structure which determines the final result. The other paradigm, the specific solvent shift for ACN in AA or TFAA, is controlled by subtle changes in the complex's intermolecular potential surface: ACN·TFAA has strongly bound linear and cyclic structures, with the deeper linear structure with the larger solvent shift preferred in the liquid, but ACN·AA has only open cyclic minima. ACN in AA thus exists as both free and bound ACN, and, despite the structure being open, the solvent shift is large (12.5 cm^{-1}), but for dilute ACN in TFAA, all ACN is bound, and there is an extremely large specific solvent shift (28.4 cm^{-1}).

Much work remains to be done in terms of determining the structures of mixtures containing ACN. Of high priority are neutron and/or X-ray structural determinations of mixed liquids, with 1:1 ACN in HOH being particularly important. Also, much could be learned from more liquid simulation studies, but, as we have seen, small changes in intermolecular energies can have profound effects on the liquid structure, and so a new generation of highly accurate intermolecular potential functions is needed. Alternatively, ACN in HOH is a good candidate for study using Carr−Parinello[83] or related a priori simulation techniques.

In terms of the quantitative interpretation of the solvent shift of associating molecules in solution, our approach here has demonstrated that, from a knowledge of the liquid structure and the intermolecular interactions which directly affect vibration frequencies, it is possible to qualitatively understand a wide range of diverse experimental data. Quantitatively, our results are not unreasonable, with, e.g., the correlation coefficient of the "observed" specific solvation and that calculated for what we believe to be the appropriate dimer structure being 0.9. An a priori computational scheme (e.g., the quantum/semiclassical dynamics scheme of Reimers, Wilson, and Heller[84]) aimed at quantitative accuracy would need to both calculate accurate liquid structures and depict the influence of these structures on the vibration frequency. Here, we used MP2 calculations for this latter task, and perhaps in the future a method could be developed to do this economically. Our MP2 calculations may serve to standardize such a method.

Finally, we note that our interest in the solvation of acetonitrile arises from the desire to interpret vibrational electroabsorption spectra for the CN stretch of ACN taken by Chattopadhyay and Boxer[85] in 2-methyltetrahydrofuran glass. Their spectral data indicate that the change in dipole moment, $\Delta\mu$, associated with the $0 \rightarrow 1$ vibrational transition in the CN stretch is 4 times our ab initio calculated value.[20] Our postulated explanation for this discrepancy is that it is due to a solvent effect, the intensity of this transition being known to range over a factor of 6 as a function of solvent. Acetonitrile, being small, extremely soluble, and absorbing in a unique spectral region, is a candidate for a local probe of electric field strength in chemical and biological systems. If $\Delta\mu$ is controlled mainly by specific solvation effects rather than by the local electric strength, acetonitrile is of no use in such an application, however. Our conclusions here, that the solvation of acetonitrile is controlled by a complex web of hydrophobic and hydrophilic interactions, indicate that, indeed, it cannot function as a reliable probe of the local electric field.

Acknowledgment. The authors gratefully acknowledge support from the Australian Research Council. We thank Dr. Bradley Collins for taking the Raman spectra and Professor Noel S. Hush for inspiration and extensive discussion of the manuscript.

Supporting Information Available: MP2/cc-pVDZ- and/or B3LYP/cc-pVDZ-calculated structures, coordinates, energies, Mulliken charges, harmonic vibration frequencies and normal modes for 92 ACN complexes, 45 monomer isomers, and AA_2 and $TFAA_2$; these structures include those as described in Figure 2 and/or Table 5, plus others (PDF). This material is available free of charge via the Internet at http://pubs.acs.org.

JA983878N

(83) Silvestrelli, P. L.; Bernasconi, M.; Parrinello, M. *Chem. Phys. Lett.* **1997**, *277*, 478.
(84) Reimers, J. R.; Wilson, K. R.; Heller, E. J. *J. Chem. Phys.* **1983**, *79*, 4749.
(85) Chattopadhyay, A.; Boxer, S. G. *J. Am. Chem. Soc.* **1995**, *117*, 1449.
(86) *Handbook of Chemistry and Physics*; Weast, R. C., Ed.; CRC Press: Cleveland, OH, 1974.
(87) Goplen, T. G.; Cameron, D. G.; Jones, R. N. *Appl. Spectrosc.* **1980**, *34*, 657.
(88) Evans, D. F.; McElroy, M. I. *J. Soln. Chem.* **1975**, *4*, 413.
(89) Rentzepis, S. *Chem. Phys. Lett.* **1974**, *29*, 23.
(90) Koetzsch, H.-J. *Chem. Ber.* **1966**, *99*, 1143.
(91) Macdonald, D. D.; Dolan, B.; Hyne, J. B. *J. Soln. Chem.* **1976**, *5*, 405.
(92) Blandamer, M. J.; Burgess, J.; Cooney, A.; Cowles, H. J.; Horn, I. M. *J. Chem. Soc., Faraday Trans.* **1990**, *86*, 2209.